Analytical solutions for piles' lateral deformations: The nonlinear stiffness case

Analytical solutions for piles' lateral deformations: the nonlinear stiffness case

Raffaele Cucuzza[a,*], Giuseppe Devillanova[b], Angelo Aloisio[c], Marco Martino Rosso[a], Giuseppe Carlo Marano[a]

[a] *DISEG, Department of Structural, Geotechnical and Building Engineering, Politecnico di Torino, Corso Duca Degli Abruzzi, 24, Turin 10128, Italy*
[b] *DMMM, Department of Mechanics, Mathematics and Management, Politecnico di Bari, Bari, Italy*
[c] *Department of Civil, Construction-Architectural and Environmental Engineering, Università degli Studi dell'Aquila, L'Aquila, Italy*

Abstract

Design of piles under lateral loads requires accurate estimation of the pile deflections. The Winkler beam model is the most popular mechanical model for piles, employed by both researchers and engineers. However, it assumes a constant soil stiffness, which is unrealistic since experimental data, referred to homogeneous soils, prove a nonlinear trend of the soil stiffness with depth. This paper discusses the limits of existing pile models and proposes an unprecedented analytical model for piles under lateral loads embedded in soils with stiffness that does not linearly depend on depth. The analytical solution of the governing Ordinary Differential Equation is derived and represented in explicit closed-form in terms of generalized hypergeometric functions. In addition, the paper delivers parametrized solutions for typical load conditions where a horizontal force and bending moment are applied at the pile's top.

The paper examines a pile response in three cases assuming as soil stiffness the constant, linear and cubic fitting of experimental estimates of the subgrade stiffness of an actual clay deposit. No negligible difference in displacement, moment and shear were detected. Still, the proposed nonlinear model leads to the most conservative estimates of the displacement. Peculiar trends characterize the results in shear and bending moment responses compared to the constant and linear soil profiles.

Keywords: Winkler model; Elastic foundation; Pile design; Analytical solution; Boundary value problem; nonlinear elastic foundation

1. Introduction

Piles are widely used to support laterally loaded structures, such as bridges, buildings, tanks, and wind turbines (see, e.g., Basu et al. [1], Filipich et al. [2], C. Zhang et al. [3], [4]). In the last two decades, several authors investigated the structural response of single and grouped piles in homogeneous and inhomogeneous soil (Mylonakis et al. [5], [6], [7], [8], Di Laora et al. [9] and Crispin [10]). There are three main methods for estimating the lateral response of piles: analytical, finite-differences or finite-elements models. Several analytical methods have been developed for analyzing piles, including the elastic subgrade reaction approach by Matlock and Reese [11], Davisson and Gill [12], or the elastic continuum approach by Poulos and Davis [13], Iancu-Bogdan Teodoru [14], Shen and Teh [15]. Nonetheless, the subgrade reaction approach, based on the Winkler foundation model, is the most widely used due to its fascinating mathematical clarity, particularly in the design practice of continuous foundations (see, e.g., Selvadurai [16]).

Terzaghi [17] observed that the modulus of subgrade reaction should be constant with the depth for clays, whereas it should increase linearly with depth for sands (see, e.g., Rowe [18]). On the other hand, the power series expression of the solution in practice provides just an approximate solution since the boundary conditions at the top of the pile can hardly be exactly satisfied if one reduces to a finite sum the power series. Moreover, preserving more terms in the power series leads to a remarkable computational effort. Within analytical approaches, several techniques based on energy principles and/or multi-layer approximations of inhomogeneous soil were developed (see e.g. Karatzia and Mylonakis [19], [20], Mylonakis et al. [6], [21]).

*Corresponding author.
Email addresses: raffaele.cucuzza@polito.it (Raffaele Cucuzza), giuseppe.devillanova@poliba.it (Giuseppe Devillanova), angelo.aloisio1@univaq.it (Angelo Aloisio), marco.rosso@polito.it (Marco Martino Rosso), giuseppe.marano@polito.it (Giuseppe Carlo Marano)

Complying with this approach, Shadlou and Bhattacharya [22] developed an elasto-dynamic solution of the pile-soil system under dynamic loading in which Hamilton's principles has been employed.

Finite-differences and finite-elements solutions can be very close to the actual solution if a sufficient number of segments are used, as demonstrated by Chen et al. [23]. However, the computational efficiency can be relatively low, especially when the pile is rather long and, as a consequence, a large number of segments is needed (see, e.g., Gao et al. [24]). However, approaches based on finite-differences or finite-elements methods are mainly used for complex soil-pile interaction phenomena (see, e.g. Nikodỳm et al. [25], Reese [26], Auersch [27]), including nonlinear effects due to soil and pile plasticization and damage or specific load patterns (see, e.g., Toscano Corréa et al. [28], Tsiatas [29], Seong-Min Kim [30]). This paper focuses on the lateral response of piles in the elastic response range. These situations are widespread in structural engineering since the foundations are also expected to remain elastic under extreme loads. Therefore, many scholars formulate the static analysis of piles under lateral loads within the elasticity theory following a continuum-based approach. This approach (see e.g. Basu et al. [31]) seems to be reliable for predicting the peak moment values, except for the function provided by Budhu and Davies [32].

Starting from the second half of the nineteenth century, several research studies dealt with the static analysis of beams lying on elastic foundations and found many engineering applications such as the design and assessment of ballasted railway tracks, beam trusses, pipelines, piles subjected to horizontal loads, shallow foundations, buried structures, floating structures (see, e.g., Hetényi [33]). In such applications, the interaction of the structure with the foundation usually named support or substratum, still represents a non-trivial problem and plays a crucial role in affecting the structural response to a given load (see, e.g., Kerr [34]), both in the static and in the dynamic ranges. Therefore, it is necessary to face the challenging problem of analyzing the response of structures lying on elastic supports, especially under spatial variations of the elastic support behaviour. In the literature, as long as the support is assumed to be homogeneous, isotropic and with a linear elastic behaviour, the in-

teraction with the structure is estimated by considering two foundation models (see Hetényi [33]): continuous medium models and the so-called "mechanical" models. The approach in the former models originates from full-scale approaches that consider a semi-infinite elastic continuum support. The models in the latter approach exclude the substratum from the analysis and reduce the problem to a suitable beam's differential equation, which includes the contribution from the foundation reaction. Mechanical models are adopted when the goal is to estimate the beam response. It is worth noting that, while the continuous approach usually becomes unsuitable since the analysis turns out to be excessively cumbersome, the second approach may be affected by oversimplified assumptions, which sometimes may not be fully representative of actual situations. Nevertheless, the latter approach may describe the structure–substratum interaction in multiple practical cases.

Past and recent experimental tests [35–44], in particular flat dilatometer tests in homogeneous soil deposits (See Fig.1), showed that the soil stiffness varies with the depth following two different trends. In the first meters, the soil stiffness increases following a positive power-like function with an exponent higher than one. Conversely, at higher depths, it stabilizes at an almost constant value following a power-like function with an exponent less the one. Since most pile foundations do not exceed a 20/30 meter depth, [45], in many practical circumstances, the subgrade stiffness is better fitted by power functions with an exponent higher than one. Therefore, the research question is: What is the approximation in linear models rather than high-order ones in estimating the lateral pile response in medium-size piles? This question can be answered using a numerical approach by selecting specific piles and soil scenarios and assessing the engineering implications of using more accurate soil models. However, this approach lacks any generalization attempt. Accordingly, the authors endeavoured to provide a general formulation for the lateral response of medium-size piles following an analytical approach. The analysis aims to foster theoretical aspects while highlighting the inherent physical meanings.

The present paper derives a mechanical model for piles under lateral loads when the subgrade stiffness has a nonlinear dependence on depth and can be described by a power function with a positive exponent. Parallelly, it discusses the practical

consequences of using a more accurate soil model by referring to an actual clay deposit.

Hence, the paper aims to obtain an analytical solution for the specific analysis of a simply-supported Euler–Bernoulli elastic beam resting on a Winkler-type elastic foundation under a static lateral load and bending moment applied at the top. Furthermore, the influence of the mechanical parameters of the beam-foundation system on the modifications of the beam elastic response is analyzed.

The following section identifies the novelty and elements of originality of the proposed pile model by reviewing the recent progresses in this field.

The paper has the following organization. Section 2 reviews the main achievements in pile modelling by introducing the elements of novelty of the proposed model. Section 3 presents the formulation of the mathematical problem and provides closed-form solutions using hypergeometric functions. A synoptic chart which summarizes the governing equations adopted into the mathematical formulations have been collected (while the details are postponed in Appendix A). Section 4 formulates the proposed pile model by highlighting existing pile models' limits. Section 4 deals with the parametric analyses, while Section 5 discusses the model limits by comparing the pile deflection in three sample cases. A final discussion and future developments will be provided in Section 6. Finally, Appendix A is devoted to the mathematical derivation of the analytical solution of the introduced model, subjected to the two point boundary conditions see Eq.(3) and Eq.(3.1.2), while in Appendix B the calculations derived by the authors for the validation, obtained by using the Symbolic Math Toolbox [46] instead of Wolfran Mathematica [47] used in [48], are exposed.

2. Literature background

In the attempt to develop a theoretical, physically reliable and, at the same time, mathematically simple representation of the elastic support, various foundation models and computational tools for structures supported along their longitudinal axis have been proposed in the literature. The well-known Winkler model (Winkler [49]) represents one of the most common approaches employed by researchers and engineerings for the evaluation of the static and dynamic soil response (Anoyatis

George and Lemnitzer Anne [50], Prendergast et al. [51], Hirai et al. [52]). According to this, the Winkler model was able to describe the reaction of the foundation system considering elastic support of a continuous array of vertical, closely-spaced, mutually-independent, linear elastic springs, which exhibits the same behaviour in tension and compression. The derived expression describing the relation between distributed reaction force q, provided by the elastic support, and the deflection of beam v, as a function of longitudinal coordinate x, is the following:

$$q(x) = K(x)v(x), \qquad K(x) > 0, \tag{1}$$

where $K(x)$ is the modulus of subgrade reaction simulating the elastic support stiffness. With the traditional approach, the previously mentioned stiffness value was assumed as constant $K(x) = K$, considering the foundation as being equivalent to an ideal fluid and $K(x)$ as its specific weight (see, e.g., [34]).

The study of beams resting on Winkler's elastic foundations has received considerable attention for over a century. However, its application was limited to prismatic beams on homogeneous foundations. Timoshenko [53] developed analytical solutions for the lateral deflection and twisting of rails under the action of statical load using Winkler's model. Biot has compared the results obtained by considering a continuous elastic approach and the Winkler model (see e.g. Biot [54]).

Several expressions for $K(x)$ are summarised in Anoyatis and Lemnitzer [50] and Shadlou et al. [55]. Other studies were developed considering Winkler-type elastic foundations with constant subgrade stiffness, see Filonenko-Borodich [56], Hetényi [33, 57], Pasternak [58], Kerr [34], and Vlasov and Leontiev [59].

Nevertheless, when various soil properties at different depths are detected, assuming constant subgrade stiffness may lead to a significant approximation error. Therefore, a few investigations on the effect of variable subgrade stiffness, $K = K(x)$, were carried out to the authors' knowledge. Initially, the Japanese structural engineer Hayashi [60] attempted to evaluate the static behaviour of a uniform beam on an elastic foundation, with stiffness value varying linearly along the beam axis, by adopting Taylor series expansion. Several contributions were derived by using

"basic" and characteristic functions in order to provide a closed-form analytical solution for a non-prismatic beam on a non-homogeneous foundation with a linear stiffness trend (Hendry et al. [61], Iyengar and Anantharamu [62], [63], Franklin and Scott [64]). Solution for stiffness values, where a positive power of x can be used $K(x) = Kx^p$, was adopted by Lentini [65] and Clastornik et al. [66]. However, it appears that there are no studies in the scientific literature related to the analytical solution for the static deformed configuration when the subgrade stiffness varies along the beam axis, with trends different than linear (see e.g. Froio et al. [67] and Darendeli et al. [68]) except for the singular case proposed by Froio and Rizzi [69]. Recently, other authors proposed general analytical Winkler solutions where generalised hypergeometric functions of the ${}_0F_3$ type are adopted with varying arbitrary values of n (see e.g. Fradelos [70], Crispin [71], Parashakis [72], Rosendo and Albuquerque [73]). Inspired by the approach in [48], in which linear dependence of the subgrade stiffness with the beam axis is adopted, an explicit closed-form analytical solution is provided herein in nonlinear dependence cases. The generalised hypergeometric functions analytically describe the solution for a beam under a force and/or a moment applied to one end. In this paper, a practical circumstance in homogeneous clay deposits and the related soil stiffness shows a nonlinear variation with depth. Therefore, analysing the beam response under nonlinear variation of the soil stiffness with depth can shed new light in the structural and/or geotechnical engineering field while simulating piles behaviour, subjected to horizontal loads and embedded in cohesionless soils (Madlhav et al. [74]) whose stiffness is nowadays still modelled as a linear function with depth (Randolph [75]). Moreover, the knowledge of analytical solutions can support, as done by Froio and Rizzi for the linear case, a parametric analysis of the beam's behaviour and its interactions with the soil in terms of variable beam's geometric and dynamic characteristics. Compared to the mathematical formulation by Froio and Rizzi, the authors propose a more generic and novel formulation that can describe different stiffness profiles simultaneously. Moreover, a clear discussion about the best model that can accurately fit the stiffness profile in a real case study is provided. The authors have embedded in a unique closed-form the traditional

Winkler model for constant subgrade modulus coefficient, the newer model derived by Froio and Rizzi for linear variation of foundation-system stiffness and the novel approach proposed by the authors considering a polynomial type dependence on the depth of the subgrade stiffness. Thus, after a parametric analysis, several variations of the beam response are depicted by considering different approximations of the soil stiffness of an actual deposit. To appreciate the final differences in the analytical solution compared to [48], the scholar can directly compare the synoptic chart in this manuscript 3.1.2 with the one provided in [48].

3. Problem definition

This paper presents a generic solution for the well-known Winkler problem by developing a general approach obtained by generalizing the formulation by Froio and Rizzi [48] from the linear to a nonlinear dependence law of the soil stifness. Several studies consider a finite free-free Euler Bernoulli elastic beam with constant cross-section resting on a Winkler foundation with an increasing subgrade stiffness with depth. This study formulates the mathematical problem for those cases where the subgrade stiffness can be approximated with a power function with exponent $n \in \mathbb{N} \setminus \{0\}$, see Fig.1.

3.1. Governing Differential Equation

In this subsection, the problem statement and the mathematical formulation of the pile's lateral deformation with nonlinear subgrade stiffness will be introduced. The transverse static deflection $v(x)$, assumed positive along the positive y direction as shown in Fig.1, of a straight Euler-Bernoulli elastic beam of length L with a constant cross-section lying on a Winkler elastic support with stiffness $K(x)$ $[F]/[L]^2$ is governed by the following 4^{th}-order Ordinary Differential Equation (ODE):

$$EJv^{(4)}(x) + K(x)v(x) = p(x), \qquad 0 < x < L, \tag{2}$$

where (formal power of a function denote the spatial derivative, of the exponent order, of the function) E and J represent, respectively, the Young's modulus of the

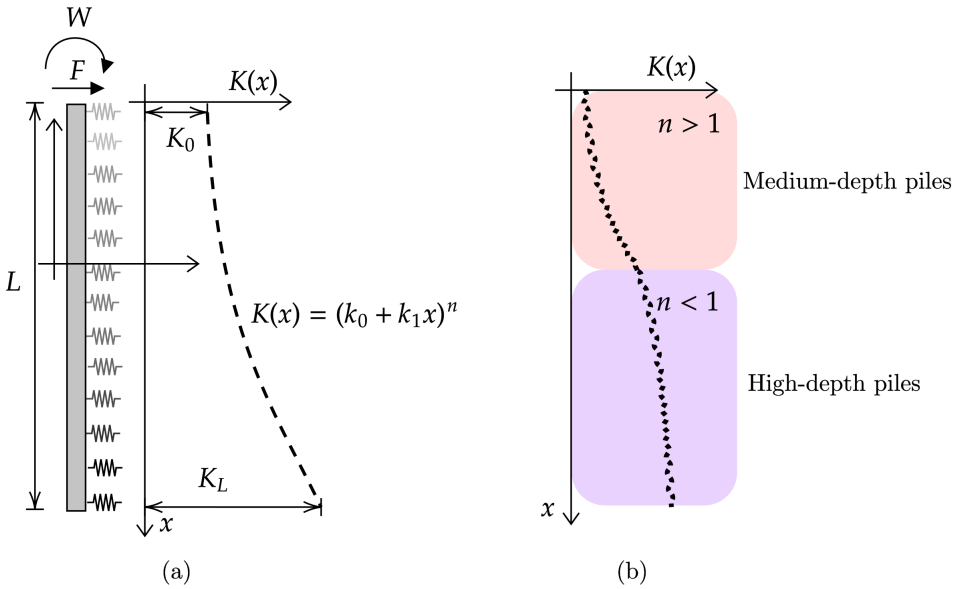

Figure 1: (a) Finite free-free Euler-Bernoulli elastic beam on winkler elastic support with power-varying stiffness coefficient $K(x)$ in the case $n = 3$. (b) Illustration of the expected trend of the subgrade stiffness for medium-length and high-length piles in homogeneous soil deposits.

beam and the moment of inertia of the beam cross-section around the z-axis while $p(x)$ $[F]/[L]$ denotes the external distributed horizontal load. By neglecting the presence of external distributed horizontal forces, i.e. by setting $p(x) = 0$, Eq.(2) reads:

$$EJv^{(4)}(x) + K(x)v(x) = 0. \tag{3}$$

$K(x)$ is described by the following polynomial function:

$$K(x) = (k_0 + k_1 x)^n \tag{4}$$

where $n \in \mathbb{N}$ is odd, k_0 and k_1 are constants such that

$$K_0 := K(0) = k_0^n \qquad K_L := K(L) = (k_0 + k_1 L)^n \tag{5}$$

are the point-wise values of the spring stiffness at the top and at the bottom ends of the beam respectively. Assumed $k_0 > 0$, the parameter k_1 must satisfy the following restriction to fulfill the physical condition $K(x) > 0$ and $K(x) \not\equiv K_0$

$$k_1 > -\frac{k_0}{L} \quad \text{and} \quad k_1 \neq 0. \tag{6}$$

3.1.1. Model Equation

In this paragraph, the general solution of the 4^{th}-order Ordinary Differential Equation (ODE) will be derived. In Appendix A we shall show that, through a suitable change of variable, Eq. (3) can be transformed into a generalized hypergeometric differential equation (see (A.4)) and that, as a consequence, Eq.(3) admits the following general solution

$$v(x) = \sum_{k=0}^{3} c_k w_k \left(-\frac{1}{(n+4)^4} \frac{(k_0 + k_1 x)^{n+4}}{EJk_1^4} \right), \quad c_k \in \mathbb{R},\ k \in \{0,1,2,3\} \tag{7}$$

where the independent solutions

$$\begin{cases} w_0(t) = {}_0F_3(-; b_1, b_2, b_3; t) \\ w_1(t) = |t|^{1-b_1} {}_0F_3(-; 2-b_1, 1+b_2-b_1, 1+b_3-b_1; t) \\ w_2(t) = |t|^{1-b_2} {}_0F_3(-; 2-b_2, 1+b_1-b_2, 1+b_3-b_2; t) \\ w_3(t) = |t|^{1-b_3} {}_0F_3(-; 2-b_3, 1+b_1-b_3, 1+b_2-b_3; t). \end{cases} \tag{8}$$

are expressed in terms of the generalized hypergeometric functions ${}_0F_3(-; b_1, b_2, b_3; \cdot)$ (see Eq.(A.5)) with $b_j = \frac{n+j}{n+4}$, $j \in \{1,2,3\}$ (see e.g. Olver et al. [76]).

In the next section we shall show how the constants c_k can be fixed by imposing a suitable two points boundary condition.

3.1.2. The two points boundary conditions

In this paragraph, the authors will define the boundary condition of the two-point Boundary Condition Problem (BVP) and a summarize all mathematical formulations in a synoptic table. The static behaviour of a uniform free-free elastic beam on a Winkler-type foundation, described by Eq.(3), subjected to lateral force F and moment W at the top-end corresponding to $x = 0$ is studied here. Therefore one is interested to the solution $v(x)$ of Eq.(3) subjected to the following Boundary

Conditions (BC):

$$\begin{cases} v_x^{(2)}(0) = -\frac{W}{EJ} \\ v_x^{(3)}(0) = -\frac{F}{EJ} \\ v_x^{(2)}(L) = 0 \\ v_x^{(3)}(L) = 0. \end{cases} \tag{9}$$

In Appendix A we shall show that the system in Eq.(9) can be transformed in the linear system

$$[B] \cdot \bar{c} = \bar{f} \tag{10}$$

in the unknown vector $\bar{c} = (c_0, c_1, c_2, c_3)^\top$, where the matrix $[B]$ is defined by Eq.(A.32) and the the vector $\bar{f}$ describing the constant terms is given as $\bar{f} = \bar{f}_F + \bar{f}_W$, where $\bar{f}_F$ and $\bar{f}_W$ are defined by Eq.(A.33) in terms of the non-dimensional parameters α and β, introduced by Eq.(11), on which the dependence of the substrate stiffness K_0 and K_L relies by Eq.(12) and Eq.(13) respectively. Then, by applying the superposition principle we get $\bar{c} = \bar{c}_F + \bar{c}_W$ with $\bar{c}_F = [B]^{-1}\bar{f}_F$ and $\bar{c}_W = [B]^{-1}\bar{f}_W$.

All calculations and the components of $\bar{c}_F$ and $\bar{c}_W$ are evaluated by using the Symbolic Math Toolbox [46]. The analytical representation is resumed in a synoptic form. Therefore, the synopsis table can be compared to the one reported in [48] for the case $n = 1$ corresponding to a linear variation of the subgrade stiffness.

Synopsis of the Analitical Solution

Governing differential equation and boundary conditions

- $EJv^{(4)}(x) + K(x)v(x) = 0; \qquad 0 < x < L; \qquad K(x) = (k_0 + k_1 x)^n;$
- $v^{(2)}(0) = -\frac{W}{EJ}; \qquad v^{(3)}(0) = -\frac{F}{EJ}; \qquad v^{(2)}(L) = 0; \qquad v^{(3)}(L) = 0.$

Definitions

- $\lambda_0 = \sqrt[4]{\frac{k_0^n}{4EJ}}; \qquad \alpha = \frac{k_0^n L^4}{EJ} = 4(\lambda_0 L)^4; \qquad \beta := \frac{k_1 L}{k_0};$
- $K_0 := K(0) = \frac{EJ}{L^4}\alpha; \quad K_L := K(L) = K_0(1+\beta)^n.$

Changes of variable

- $s = s(x) = \frac{k_0 + k_1 x}{\gamma} \iff x = x(s) = \frac{\gamma s - k_0}{k_1};$
- $t = t(s) = -\frac{s^{n+4}}{(n+4)^4} \iff s = s(t) = (-(n+4)^4 t)^{\frac{1}{n+4}};$
- $t = t(x) = -\frac{1}{(n+4)^4}\left(\frac{k_0 + k_1 x}{EJk_1^4}\right)^{n+4}.$

General solution

- $w(t) = \sum_{k=0}^{3} c_k w_k(t); \qquad b_j = \frac{n+j}{n+4}, \quad 1 \le j \le 3;$
- $$\begin{cases} w_0(t) = {}_0F_3(-; b_1, b_2, b_3; t) \\ w_1(t) = |t|^{1-b_1}{}_0F_3(-; 2-b_1, 1+b_2-b_1, 1+b_3-b_1; t) \\ w_2(t) = |t|^{1-b_2}{}_0F_3(-; 2-b_2, 1+b_1-b_2, 1+b_3-b_2; t) \\ w_3(t) = |t|^{1-b_3}{}_0F_3(-; 2-b_3, 1+b_1-b_3, 1+b_2-b_3; t). \end{cases}$$
- ${}_0F_3(-; b_1, b_2, b_3; t) = \sum_{h=0}^{\infty} \frac{1}{(b_1)_h (b_2)_h (b_3)_h} \frac{t^h}{h!}; \qquad \bar{c} = (c_0, c_1, c_2, c_3);$
- $v(x) = \sum_{k=0}^{3} c_k w_k \left(-\frac{1}{(n+4)^4}\frac{(k_0+k_1x)^{n+4}}{EJk_1^4}\right); \qquad \bar{c} = \bar{c}_F + \bar{c}_W;$
- $\bar{c}_F = [B]^{-1} \cdot \bar{f}_F; \qquad \bar{c}_W = [B]^{-1} \cdot \bar{f}_W;$
- $[B]^{-1}$ inverse matrix of $[B]$ defined in Eq.(A.32);
- $\bar{f}_F = \frac{FL^3}{(\alpha\beta^n)^{\frac{3}{n+4}}EJ}(0, -1, 0, 0)^\top; \qquad \bar{f}_W = \frac{WL^2}{(\alpha\beta^n)^{\frac{2}{n+4}}EJ}(-1, 0, 0, 0)^\top.$

4. Parametric analyses by varying α and β

A parametric analysis was performed to investigate the response of in a homogeneous soil by varying the mechanical property of the foundation and pile. The structural behavior of pile will be expressed in terms of displacement, bending moment and shear.

By solving Eq.(10), one gets the vector $\bar{c} = (c_0, c_1, c_2, c_2)$ whose components give the coefficients to be replaced in Eq.(7) to get the unique solution of the BVP (Eqs.(3)-(9)).

As already done in [48] for the linear case $n = 1$, the following non-dimensional parameters are introduced

$$\alpha := \frac{k_0^n L^4}{EJ}, \qquad \beta = \frac{k_1 L}{k_0} > -1, \tag{11}$$

(to get the inequality we have used Eq.(6)) so that the substrate stiffness $K_0 = K(0)$ in $x = 0$ is proportional to α according to the identity

$$K_0 = k_0^n = \frac{EJ}{L^4}\alpha \tag{12}$$

while the substrate stiffness $K_L = K(L)$ in $x = L$ is proportional to $(1 + \beta)^n$ according to the relation

$$K_L = (k_0 + k_1 L)^n = (k_0 + \beta k_0)^n = k_0^n (1 + \beta)^n = K_0 (1 + \beta)^n. \tag{13}$$

Therefore, given the material and geometric parameters E, J and L of the beam, multiple scenarios can be investigated in terms of the parameters α and β which, in such a case, describe different soil conditions. In order to make a strict comparison to the case $n = 1$ presented in [48], we shall also make use of the so called characteristic parameter of the system, see [33],

$$\lambda_0 := \sqrt[4]{\frac{k_0^n}{4EJ}} \quad \text{so that} \quad \alpha = 4(\lambda_0 L)^4. \tag{14}$$

Hence, it is clear that the beam response depends on the two introduced non-

dimensional parameters α and β defined by Eq.(11), which take into account not only the geometric and material features of the pile (E, J and L), but also the soil stiffness.

Since $\alpha = 4(\lambda_0 L)^4$, the authors will assume, according to the realistic range provided by Selvadurai [16] and Di Laora et al. [77], that $\lambda_0 L$ is an integer between 1 and 6, so that

$$\alpha \in [4 \cdot 1^4, 4 \cdot 6^4]; \tag{15}$$

Conversely, since β is greater than -1 and high values of β (beyond 8) simulate very stiff foundations, the authors will assume that

$$\beta \in [-0.5, 0) \cup (0, 8]. \tag{16}$$

Despite the variability range of the parameters adopted in [48], the case $\beta = -1$ is not considered since the solutions to Eq.(A.31) are not numerically determined. Several derivatives that compose the matrix $[B]$ reach singularity points when $\beta = -1$. However, another representative value equal to -0.5 is used to investigate the soil response for $\beta < 0$. Future works will investigate this special case in order to provide a dedicated mathematical analysis on the invertibility condition of the corresponding matrix $[B]$.

As observed in [48], the particular case corresponding to a constant foundation coefficient ($\beta = 0$) is obtained when $\beta \to 0$. This assumption leads to the traditional Winkler beam model well described in [48, Section 3.3].

The analytical solution of the ordinary differential equation describing the static deflection, bending moment and shear of a simply-supported vertical Euler–Bernoulli elastic beam on a variable Winkler elastic coefficient are obtained by varying α and β. Therefore, two main scenarios are analyzed, corresponding to a force (F) and to a bending moment (M) alternatively applied at the pile top. Normalization was applied to each solution in terms of static deflection, bending moment, and shear. Therefore, the following expressions for both scenarios are investigated:

$$\tilde{v}_F(x) = \frac{v_F(x)}{v_F^{max}}; \qquad \tilde{v}_W(x) = \frac{v_W(x)}{v_W^{max}}; \tag{17}$$

$$\tilde{M}_F(x) = \frac{M_F(x)}{M_F^{max}}; \qquad \tilde{M}_W(x) = \frac{M_W(x)}{M_W^{max}}; \tag{18}$$

$$\tilde{S}_F(x) = \frac{S_F(x)}{S_F^{max}}; \qquad \tilde{S}_W(x) = \frac{S_W(x)}{S_W^{max}}; \tag{19}$$

where $M_F(x)$ (or $M_W(x)$), and $S_F(x)$ (or $S_W(x)$), may be written as:

$$M_F(x) = -\frac{EJ}{L^2} v_F^{(2)}(x); \qquad S_F(x) = -\frac{EJ}{L^3} v_F^{(3)}(x), \tag{20}$$

and M_F^{max} and M_W^{max} are the respective maximum bending moment along the beam. In the parametric analyses shown in subsections 4.1 and 4.2, the variability of normalized displacement, bending moment and shear with varying coefficients α and β will be investigated for $n = 3$, complying with the real case application discussed in Section 5. As a validation of the proposed formulation, in the Appendix B the same calculation for $n = 1$ have been provided with the Symbolic Math Toolbox [46]. The results shown in Figs.B.8(a)-(f) and Figs.B.9 (a)-(f) match with those obtained by Froio and Rizzi in [48].

4.1. First case: force application

This paragraph investigates the behaviour of a pile subjected to horizontal load with varying soil properties. The results will be expressed in a normalized form, as introduced in Section 4. Figs.2(a)-(f) show the shape of the normalized elastic deflection $\tilde{v}_F$, given in Eq.$(17)_1$. The deflection is plotted against the spatial coordinate x by varying α, given β. Compared to the work in [48], the authors plot the normalized profile of each characteristic stress with respect to dimensional spatial axis complying with the pile information of the case study discussed in Section 5. As clearly defined in Eq.(11), the parameter α is representative of the ratio between the stiffness of the foundation, K_0, calculated at the top end of the beam, and the beam's bending stiffness E. The influence of these parameters is manifest in each plot shown in Figs.2(a)-(f) and, for relatively small values of α, the shape of the curves approaches the linear trend. Accurately, for $\alpha = 4$ or $\lambda_0 L = 1$, an unambiguous linear trend is recognised. This scenario perfectly simulates the situation corresponding to either a stiff beam or a soft foundation, or, in other words, the

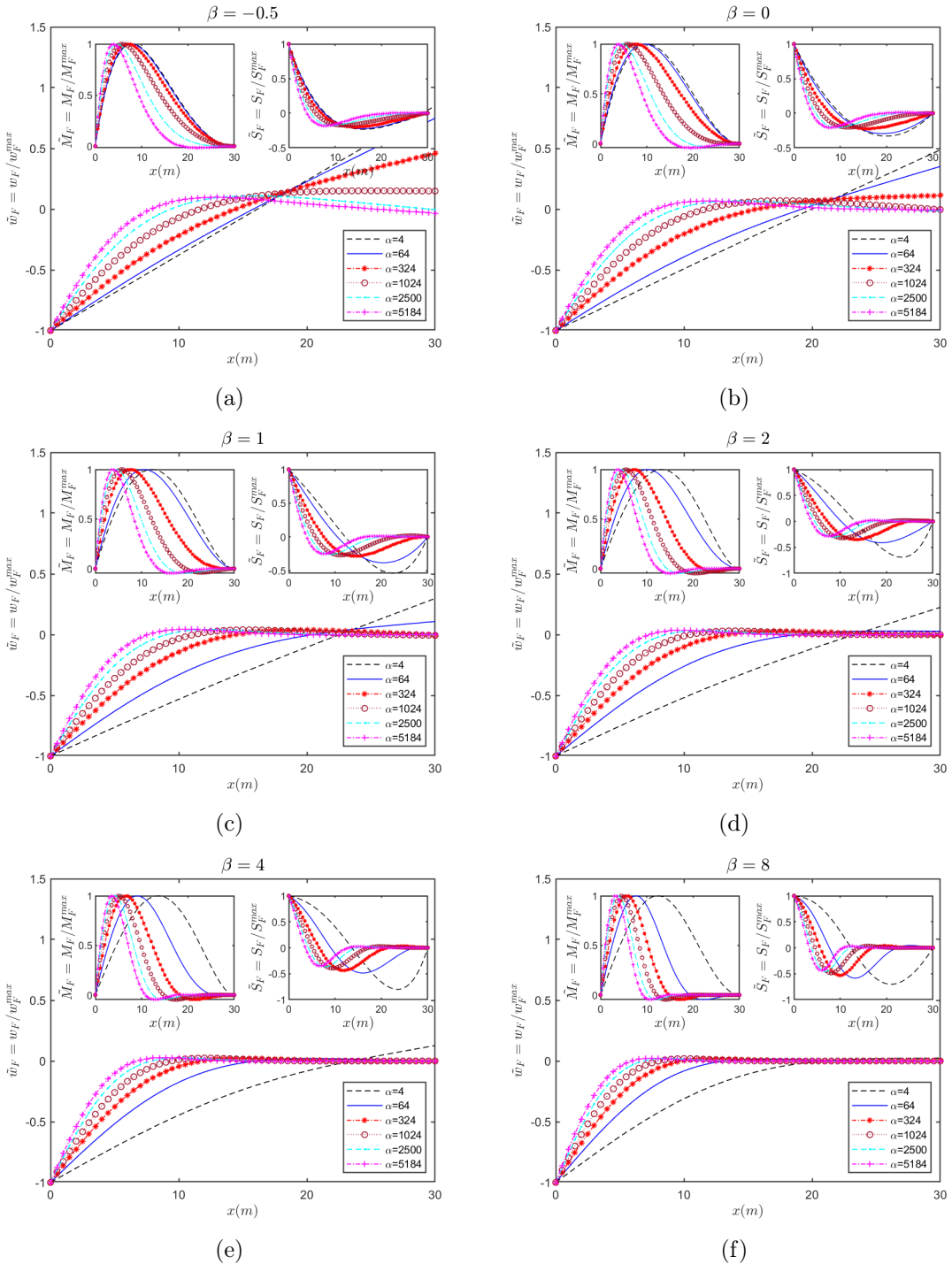

Figure 2: Normalized shape of elastic deflection $\tilde{v}_F = v_F/v_F^{max}$, bending moment $\tilde{M}_F = M_F/M_F^{max}$ and shear $\tilde{S}_F = S_F/S_F^{max}$, under horizontal force F, for various values of α and β ($\beta = -0.5$ (a), $\beta \to 0$ (b), $\beta = 1$ (c), $\beta = 2$ (d), $\beta = 4$ (e), $\beta = 8$ (f)).α is representative of the ratio between the stiffness of the foundation, K_0, calculated at the top and of the beam, and the beam's bending stiffness E. As α approaches relatively high values, the beam longitudinal axis starts deforming more, conversely for low values of the same parameter stiff foundation is simulated.β is representative of the steepness of the elastic stiffness, k_1/k_0, coefficient variation along the beam axis. For positive higher value of β, stiff foundation property is achieved early with varying beam longitudinal axis. Negative value of this parameter simulates soft soil responses with decreasing stiffness of the elastic springs at increasing depth.

Young Modulus's E rises and the initial stiffness K_0 decreases. On the other hand, for higher values of α, the static beam deflection rises, displaying an asymmetric evolution with the maximum displacement at the point of application of the force F. A very rapid decrease from the top end is detected in the above case.

Compared to the previous case, the influence of the elastic stiffness coefficient β along the x-axis is less evident. Negative values of β simulate soft soil responses with decreasing stiffness of the elastic springs and increasing depth, as depicted in Fig.2. On the other hand, small values of α are associated with a deflection plot symmetric to the pile's midspan. Conversely, higher values of α lead to a symmetry loss. Moreover, a stabilization of the family curves is recognized towards zero when positive values of β are considered (Figs.2(c)-(f)). As revealed by [48], the case for β approaching zero corresponds to the Winkler theory when the subgrade stiffness $K(x)$ is constant. The subplots placed at the left of Fig.s2 (a)-(f) show that all the normalized bending moments approach zero at the beam end. Beyond the peak values of the curves, occurring within the first half of the beam, a rapid decrease of the normalized moment becomes less noticeable with increasing values of α. The cases of soft soil ($\beta < 0$) when flexural behavior is observed (see Fig. 2(a)) does not lead to a moment inversion. Contrariwise, in the remaining cases plotted in Figs.2(b)-(f), negative normalized moments arise in the second half of the beam. As confirmed by the deflection plots, all the curves subjected to this analysis reach the maximum bending moment, M^{max}, at the top end of the beam where the force F is applied. The bending moment can be positive or negative depending on the force direction. Therefore, the scenarios corresponding to increments of α and decrements of β manifest an evident translation of the peaks towards the beam's top-end. This situation corresponds to a higher subgrade stiffness at lower depths. Finally, the variation between scenarios seems to be more pronounced by varying α versus β. Hence, the bending moment is susceptible to the foundation system's initial stiffness or to the pile's material property. As expected, for low values of α, the evolution of bending moment approaches a quartic polynomial profile according to the static response of a rigid beam.

The subplot located at the left of Figs.2(a)-(f) display a representation of the

parametric evolution of the normalized shear $\tilde{S}_f$. The maximum absolute shear acting on the beam is attained at the top-end where $S_F^{max} = F$. The effect of external load F rapidly decreases, moving away from the application point. Moreover, when a rigid foundation system or flexible beam is investigated (for increasing values of α), the negative peak value becomes more evident and moves towards the beam's top end. Therefore, a rapid decay to zero of the normalized shear is identified when α and β increase. For small values of α and imposing $\lambda_0 L = 1$, the profile of the curves approximates a cubic power function. This plot is close to the shear diagram of a rigid beam on a Winkler foundation. The trend of the curves, especially for Fig.**??**, shows that in soft foundation systems, the normalized shear approaches zero without any change of concavity, except for the beam's bottom-end. Conversely, for rigid soils (high values of K_0), the effect of external load vanishes at the midspan of the beam.

The main difference with respect to [48] is related to the negative value investigation for β. The singularity case when $\beta \to -1$ deserves a dedicated mathematical formulation. This latter aspect is of great interest since reproduces the limit case of the absence of foundation, as observed in [69]. With particular reference to $\beta = 8$ the reduction of the beam displacements towards zero, in the second half of the beam, becomes more evident with respect to case study $n = 1$.

4.2. Second case: Bending moment application

To provide further validations of the proposed model, a beam subjected to a moment W applied at its top end, as discussed in [48], is analyzed. Results will be expressed in a normalized form, as introduced in section 4. The normalized shape of elastic deflection $\tilde{v}_W$, defined in Eq.$(17)_2$, versus dimensional spatial coordinate x is evaluated by varying, as described in Section 4.1, the parameters α and β. The plot of the curve profiles are depicted in Fig.3. Consistently with the previous case study, a linear deflection profile is recognised with low values of the parameter α. On the contrary, when α increases, the maximum positive value of curves is reached more rapidly compared to the applied force case. Moreover, increasing β, the profile of the curve tends to rapidly approach zero. The solution exhibits low oscillations around

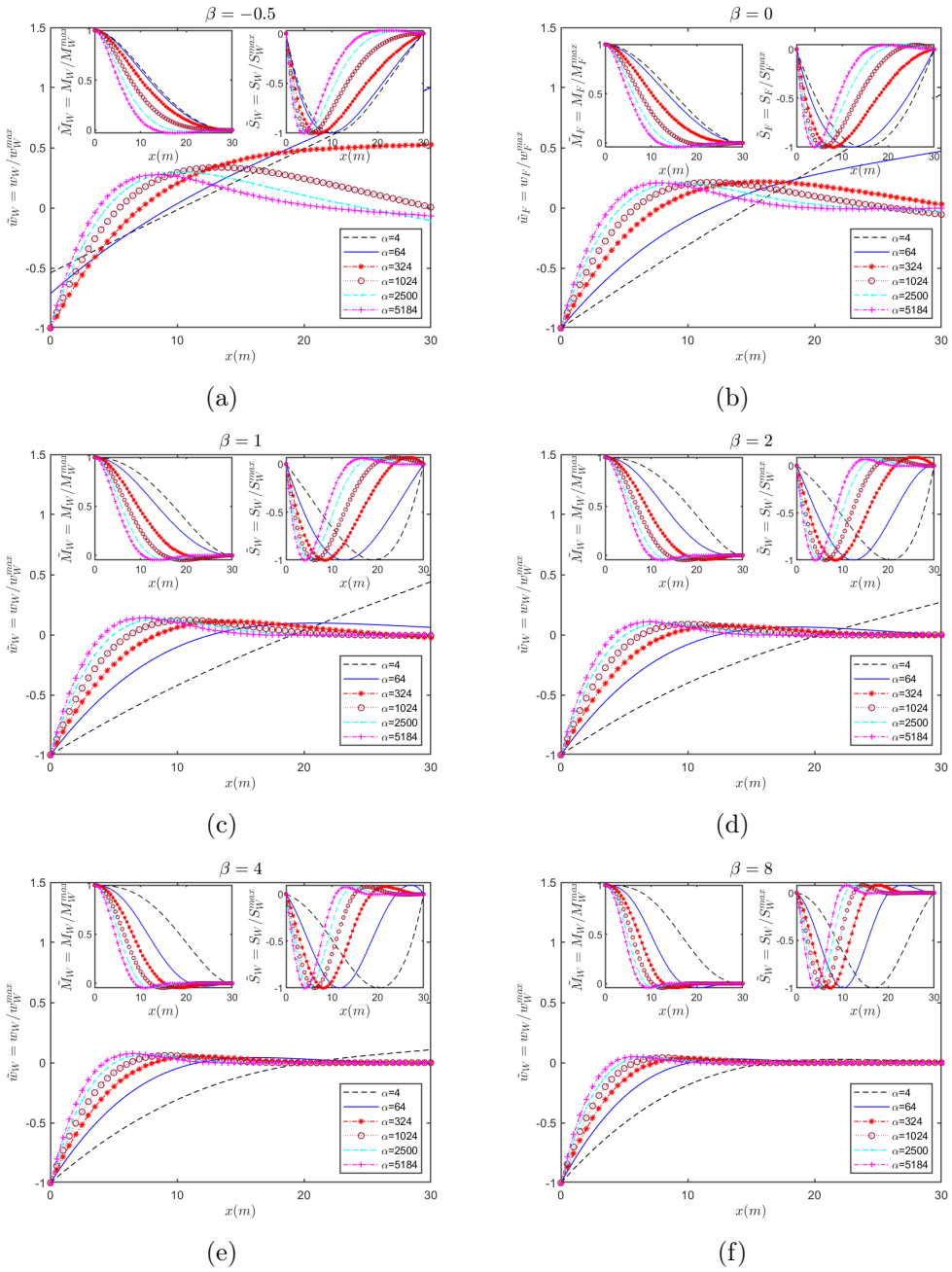

Figure 3: Normalized shape of elastic deflection $\tilde{v}_W = v_W/v_W^{max}$, bending moment $\tilde{M}_W = M_W/M_W^{max}$ and shear $\tilde{S}_W = S_W/S_W^{max}$, under moment W, for various values of α and β ($\beta = -0.5$ (a), $\beta \to 0$ (b), $\beta = 1$ (c), $\beta = 2$ (d), $\beta = 4$ (e), $\beta = 8$ (f)).α is representative of the ratio between the stiffness of the foundation, K_0, calculated at the top and of the beam, and the beam's bending stiffness E. As α approaches relatively high values, the beam longitudinal axis starts deforming more, conversely for low values of the same parameter stiff foundation is simulated.β is representative of the steepness of the elastic stiffness, k_1/k_0, coefficient variation along the beam axis. For positive higher value of β, stiff foundation property is achieved early with varying beam longitudinal axis. Negative value of this parameter simulates soft soil responses with decreasing stiffness of the elastic springs at increasing depth.

the same value in the proximity of the second-half beam. Concerning the curves with negative values of β, the maximum displacements for $\alpha = 4$ and $\alpha = 64$, as shown in Fig.3(a), approach the y-axis at -0.7 and -0.5 respectively. Concerning flexural Behaviour depicted in subplots of Fig.s 3 (a)-(f) , the maximum moment for each investigated scenario is achieved at the application point of the bending moment. For higher values of either α and β, the sigmoid shape of the curves becomes more evident with a trend that decays faster, moving away from the application point. Compared to the first load case with a top force F, the concavity change occurs twice instead of once. Negative moments are observed for either high values of α or low values of β due to the increasing soil stiffness towards the beam bottom. On the contrary, when higher values of β occur, all curves approach zero in the first half of the beam except for $\alpha = 4$. Finally, the parametric trend of normalized shear $\tilde{S}_W$ is shown on the right side of Fig.3. The shear force for each scenario reaches a null value at the top-end of the beam. Conversely, the maximum shear is detected at the first half of the beam for high soil stiffness. The maximum shear moves at the second half of the beam for either a higher value of α or β. As shown in the first load case with a top force application, the results obtained by the authors are consistent with those obtained by [48]. Main differences between the two models are recognized when curves approach to zero, in fact for increasing value of β the null value is reached rapidly for $n = 3$. For these reasons, the mentioned approach can be considered a peculiar case of a broader mathematical formulation herein exposed. Hence, a pile embedded in soil with a nonlinear stiffness variation with depth is considered in the next section. The case study is based on actual data referred to a homogeneous clay deposit where the best fit of the soil stiffness with depth is obtained with $n > 1$, (see 1).

5. Discussion and real case application

The parametric analyses presented in the above section refer to general cases. In this section, the authors consider an actual profile of the subgrade stiffness, characterized by a marked nonlinear trend. Homogeneous clay deposits manifest a nonlinear increment of the subgrade stiffness with depth. Specifically, the authors

considered the geotechnical parameters identified in the homogeneous clay deposit of the Fucino basin (Italy). The geotechnical parameters estimated in a vertical axis of the Fucino basin (Italy) are used to estimate the subgrade coefficient up to 30 m depth. The values of the subgrade coefficient are fitted using a power function using a Lovemberg-Marcquard optimization algorithm. The fitting function allows assessing the effects of a variable subgrade coefficient in an actual case. The homogeneity of the clay deposit endorses its use to compare the pile response in three cases:

- a constant subgrade stiffness is considered, corresponding to the average value in the considered 30m depth;
- a subgrade stiffness linearly increasing with depth;
- a cubic power function of the subgrade stiffness, obtained by fitting the experimental estimates of the soil stiffness.

The three cases correspond to a progressive refinement of the soil model and allow to compare the approximation corresponding to the use of the simple-Winkler beam model or a subgrade stiffness linearly increasing with depth, following the approach by [48], up to a cubic dependence from depth of the foundation stiffness. Therefore, the mathematical formulation adopted by calculating the soil stiffness in the case of $\beta = \gamma = k_1 = 0$, corresponding to the simple-Winkler beam model, was inspired by [48] (chapter 3.3 "Singular case") by taking $n = 1$ in $\gamma = \sqrt[4]{\frac{k_0^n}{4EJ}}$,
The following subsection briefly introduces the geological nature of the deposit and the experimental results used for estimating the evolution of the subgrade coefficient with depth.

5.1. Site description and geotechnical characterization

The Fucino basin is a Quaternary tectonic depression located in the core of the central Apennines of Italy. Seismic reflection data reveal a half-graben sedimentary infill in the hanging wall of the Fucino fault, with Quaternary sediments recording a maximum thickness of approximately 1000 m [78].
There are three primary stratigraphic successions in the Fucino area, described by the Geological Map of Italy:

- The first succession includes old fluvial and lacustrine deposits, with thick interlayers of slope-derived massive rocks, which outcrop on the northern and northeastern sides of the basin.

- The second succession characterizes the marginal area of the lacustrine depression, where fine-grained lacustrine sediments (silt and clay) are interbedded with coarse-grained (sand and gravel) alluvial, deltaic and shoreline deposits.

- The third succession characterizes the central part of the basin; its stratigraphy is dominated by fine-grained lacustrine sediments (silt and clay), with increasing proportions of sand layers in the areas closest to the margins.

The experimental analyses focused on the third succession, dominated by clay with interbedded sand lens.

The geotechnical parameters of the deposit are obtained by using the mechanical flat dilatometer (DMT) [79–82]. The flat dilatometer is a steel blade with dimensions 95×200×15 mm, ending with a sharp lower edge. One side of the blade exhibits a circular steel membrane, which is expanded during the test. The pressure readings allows to evaluate the following geotechnical parameters: Oedometer modulus (both in cohesive and cohesionless soils), M, Undrained shear strength (cohesive soils), S_u, in situ earth pressure coefficient (cohesive soils), K_0, Overconsolidation ratio (cohesive soils), OCR, Friction angle (cohesionless soils), ϕ, Unit weight, γ. The Oedometer modulus (M) can be used to estimate the subgrade coefficient, by multiplying its value by the pile diameter.

Fig.4 plots the experimental estimates of the Oedometer modulus with depth, the linear and nonlinear fitting of the experimental data using a cubic power function. The data shown in Fig.4 prove that the Oedometer modulus exhibits a marked nonlinear trend. After a superficial sandy layer, the soil is prevalently clay. The Oedometer modulus, starting from values equal to 1 MPa, attains values close to 6 MPa at approximately 30 m depth. The equation reported below leads to a satisfactory fitting of the experimental data, with a correlation coefficient R^2 equal to

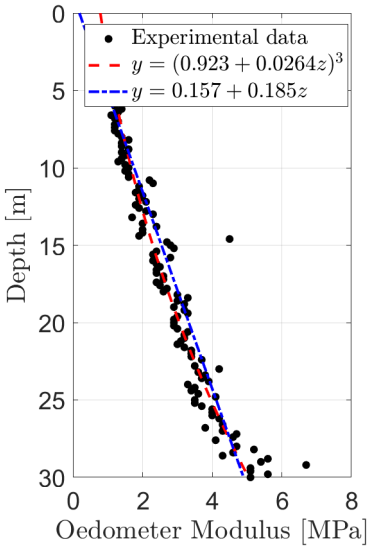

Figure 4: Experimental estimate of the Oedometer modulus and fitting with a cubic power and linear functions.

0.88 and a root mean square error (RMSE) equal to 0.49.

$$K(x) = (0.923 + 0.0264x)^3. \tag{21}$$

The authors observed that the best fitting is obtained with $n = 3$. A linear fitting is associated with a $R^2 = 0.81$ and RMSE=0.56.

With the aim to adapt the previous parametric analysis to the real case application, a calibration phase must be conducted by fixing the geometric and material characteristic J, L and E of the pile and the soil property (α and β coefficients) with the following expressions:

$$\alpha = \frac{K_0 L^4}{EJ}; \qquad \beta = \frac{K_L^{\frac{1}{n}} - K_0^{\frac{1}{n}}}{K_0^{\frac{1}{n}}} \tag{22}$$

where n=3, K_0 is equal to $(0.923)^3$ and K_L is equal to $(0.923{+}0.0264L)^3$. The length of the pile, L, is assumed as equal to the considered 30 m depth for geotechnical investigations.

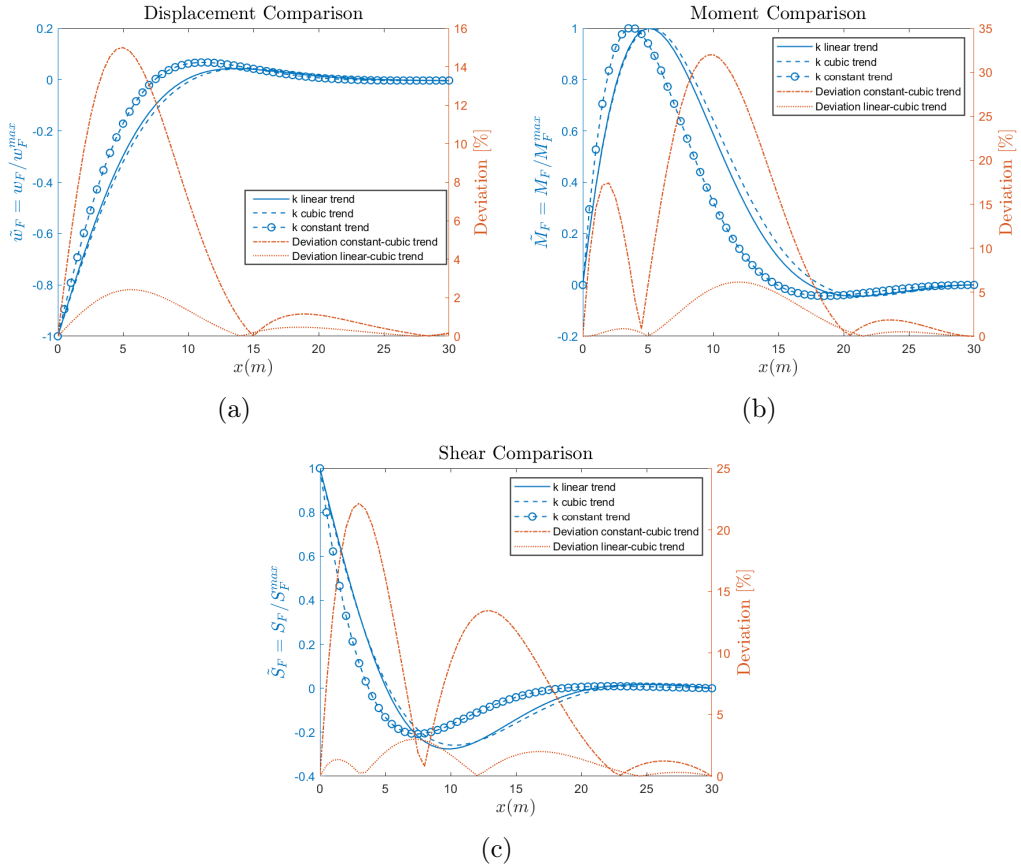

Figure 5: Comparison between displacement (a), bending moment (b) and shear (c) associated with cubic, linear and constant stiffness trend respectively for a pile subjected to force F at the top-end. The left y-axis shows the normalized deflection, bending moment and shear, while the right y-axis the differences between the cubic-linear and cubic-constant models of the subgrade stiffness. x-axis is representative of the pile's depth measured in meters [m].

5.2. Parametric analyses using the experimental fitting

In this paragraph, some comparisons between different subgrade stiffness trends will be provided adopting the analytical model proposed by authors. Figs.5-6 plot the deflection, bending moment and shear of three soil-beam interaction models, associated with a constant, linear and cubic increment of the subgrade stiffness. Specifically, Figs.5-6 show the results referred to a horizontal force and to a bending moment applied at the pile's head, respectively. The left y-axis shows the normalized deflection, bending moment and shear, while the right y-axis the differences between the cubic-linear and cubic-constant models of the subgrade stiffness. The main aspects arising from the direct observation of Fig.5 and Fig.6 are:

- The overall trend of the static deflection is comparable between the three mod-

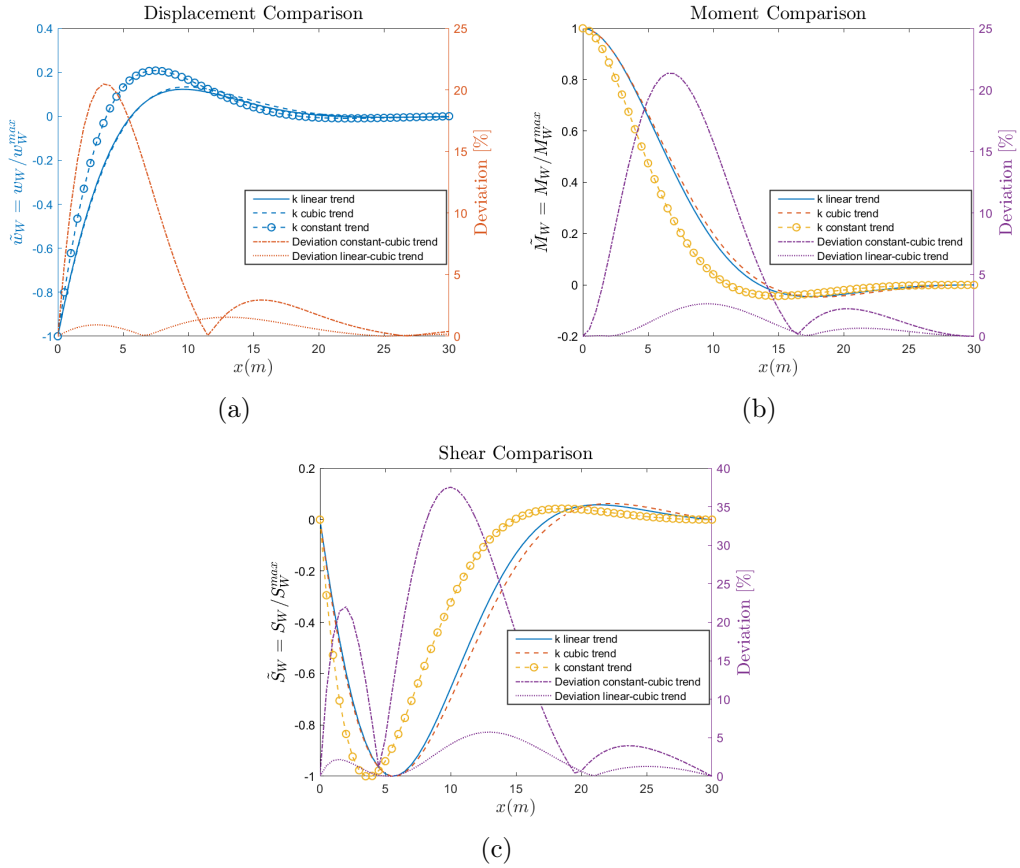

Figure 6: Comparison between displacement (a), bending moment (b) and shear (c) associated with cubic, linear and constant stiffness trend respectively for a pile subjected to moment W at the top-end.The left y-axis shows the normalized deflection, bending moment and shear, while the right y-axis the differences between the cubic-linear and cubic-constant models of the subgrade stiffness. x-axis is representative of the pile's depth measured in meters [m].

els. However, the Winkler beam model leads to an evident underestimation of the beam deflection for either piles' investigations. The maximum discrepancy, close to 14%, is reached after attaining the force application point, close to the inversion point. Conversely, the discrepancy between the linear and cubic models is minor. The linear model overestimates the beam deflection, with a maximum error close to 2%.

- The percentage difference between the results of the two models in terms of static deflection, bending moment and shear has two local maxima, close to the pile edges. The local maximum close to the force application point is more prominent than the second one. There is a central region where there is no meaningful difference between the three models at approximately half the pile

length.

- The evolution of the bending moment is similar between the three models for either pile's configurations. However, the Winkler model is associated with a shift towards the pile top. The Winkler model causes a shift of the maximum closer to the ground surface. The percentage difference between the three models is higher respect to the ones obtained for the static deflection. The maximum difference between the bending moment in the constant-cubic cases reaches the 32% when pile is subjected to force F at the top-end. Moreover, when the curve related to the Winkler model approaches the linear or cubic ones (see Figs. 5-(b)), the deviation approaches zero. In the above mentioned cases, difference between the three different analytical methods is null. Generally, Winkler model leads to underestimate the flexural response of the pile respect cubic or linear profile when force F and moment W act.

- The plots in terms of shear forces have a similar trend. However, with regards to the investigated case in which pile is subjected to force, Fig.5-(c), the shear force obtained from the Winkler model is underestimated compared to the other models independently by the pile's depth. On the contrary, when shear behaviour of pile subjected to moment is observed, Fig.6-(c), shear profile associated with Winkler model results being given an overstimate of measure respect the other models. Instead, an underestimation is recognized among the first and second null point of the deviation profile. Additionally, the shear diagram of the Winkler model is likely to be shifted towards the pile top. Therefore, the minimum point is attained closer to the ground level. The maximum percentage differences between the cubic-linear and cubic-constant cases are 5% and 37%, respectively.

In conclusion, some general considerations derived from the two investigated scenario. Applying a bending moment leads to a higher discrepancy between the three models. Specifically, the maximum discrepancy of the cubic-constant reach 22%, 32% and 37% for the deflection, bending moment and shear, respectively. The maximum difference between the cubic-linear is approximately 2-5%, as manifested in

Fig.s (5)-(6).

The comparison in Fig.s (5)-(6) prove that the constant, linear and cubic models for the subgrade stiffness lead to a progressive enhancement of the model prediction. However, the improvement in the model accuracy obtained for the cubic subgrade stiffness become less evident when the comparison with linear subgrade stiffness is investigated. Generally, the Winkler model with constant stiffness coefficient leads to a clear underestimation of beam deflection for each considered scenario. However, when the bending moment or shear, associated with the constant profile, approaches the curves related to cubic or linear profile (see Figs.5(b)-(c) or Fig.6(c)) the trend is inverted. Specifically, the curves related to cubic or linear profiles exhibit higher values of moment and shear. Therefore,when the beam is subjected to a top bending moment, the percentage deviation between constant and cubic trends becomes more evident.

6. Conclusions and future developments

In the present analysis, a general, closed-form solution for the static elastic deflection of a free-free Euler-Bernoulli beam on Winkler support with positive power variation stiffness along the beam axis under force and/or moment applied at one of its edges has been proposed.The analytical model was obtained by generalizing to the nonlinear case the well-known formulation proposed by Froio and Rizzi in [48] of the linear dependence of the subgrade stiffness. The expression of the general integral, the changes of variable adopted, and the solution of the Boundary Value Problem governed by a linear differential equation with variable coefficients have been derived (see Appendix A) and clearly summarized in the synoptic chart 3.1.2. First, the problem definition and the mathematical formulation have been outlined. Then, a complete parametric analysis with suitable varying parameters was performed in order to verify the consistency of the authors' achievements with the results shown in Literature for similar case. A detailed description of the plot for each scenario has been provided with particular attention to singularity cases.
Finally, a real case application was investigated, adopting an actual profile of the subgrade modulus, characterized by a marked nonlinear trend. Using the proposed

mathematical formulation, three different models (constant, linear and cubic power stiffness profile) have been analyzed to compare percentage variation between curves. Several fundamental findings in the behaviour of the beam-support mechanical system arose from the discussion of results:

- A general expression for the solution of the boundary value problem, based on the theory of Ordinary Differential Equation, has been provided for a non-linear trend of the subgrade stiffness.The proposed formulation also describes singularity cases, like the case of negative steepness of the subgrade stiffness.

- The linear case, studied by Froio and Rizzi [48], can be considered as a degenerate case of the proposed formulation. Results was re-obtained by the author and reported in Appendix B for completeness and comparison purposes when $n = 1$.

- The validation of the mathematical formulation for a real case application reveals that the linear and cubic stiffness profiles are more conservative than the constant one when the beam's displacement has been investigated. Instead, the constant subgrade coefficient represents the stricter requirement only at the top beam when the structural design has been performed to bending moment and shear.

For all these reasons, the considered case study may constitute a benchmark case for validating the reliability and accuracy of alternative numerical approaches and/or give some preliminary indications to engineers in the practical design of beams on nonlinear Winkler foundations.

In future developments, the case $\beta \to -1$ will be derived in order to provide a complete and exhaustive generic mathematical formulation of the Boundary Value Problem. Furthermore, a comparison between results obtained by the analytical model and site tests could be estimated to check the model's accuracy in real case applications.

Data availability statement

Some or all data, models, or code that support the findings of this study are available from the corresponding author upon reasonable request.

References

[1] D. Basu and R. Salgado, "Analysis of laterally loaded piles with rectangular cross sections embedded in layered soil," *International Journal for Numerical and Analytical Methods in Geomechanics*, vol. 32, no. 7, pp. 721–744, 2008.

[2] C. P. Filipich and M. B. Rosales, "A further study about the behaviour of foundation piles and beams in a winkler–pasternak soil," *International journal of mechanical sciences*, vol. 44, no. 1, pp. 21–36, 2002.

[3] G. Gholipour, C. Zhang, and M. Li, "Effects of soil–pile interaction on the response of bridge pier to barge collision using energy distribution method," *Structure and Infrastructure Engineering*, vol. 14, no. 11, pp. 1520–1534, 2018.

[4] W. D. Guo, *Theory and practice of pile foundations*. CRC press, 2012.

[5] G. Mylonakis and G. Gazetas, "Lateral vibration and internal forces of grouped piles in layered soil," *Journal of geotechnical and geoenvironmental engineering*, vol. 125, no. 1, pp. 16–25, 1999.

[6] G. Mylonakis and D. Roumbas, "Lateral impedance of single piles in inhomogeneous soil," 2001.

[7] G. Mylonakis, "Elastodynamic model for large-diameter end-bearing shafts," *Soils and foundations*, vol. 41, no. 3, pp. 31–44, 2001.

[8] G. E. Mylonakis and J. J. Crispin, "Simplified models for lateral static and dynamic analysis of pile foundations," in *Analysis of Pile Foundations Subject to Static and Dynamic Loading*, pp. 185–245, CRC Press, 2021.

[9] R. Di Laora and E. Rovithis, "Kinematic bending of fixed-head piles in nonhomogeneous soil," *Journal of Geotechnical and Geoenvironmental Engineering*, vol. 141, no. 4, p. 04014126, 2015.

[10] J.J.Crispin, "Static and dynamic analysis of piles in inhomogeneous soil," *PhD. Thesis*, no. University of Bristol, p. UK, 2022.

[11] H. Matlock and L. C. Reese, "Generalized solutions for laterally loaded piles," *Journal of the Soil Mechanics and foundations Division*, vol. 86, no. 5, pp. 63–92, 1960.

[12] M. Davisson and H. Gill, "Laterally loaded piles in a layered soil system," *Journal of the Soil Mechanics and Foundations Division*, vol. 89, no. 3, pp. 63–94, 1963.

[13] H. G. Poulos, E. H. Davis, *et al.*, *Pile foundation analysis and design*, vol. 397. Wiley New York, 1980.

[14] I.-B. Teodoru, "Beams on elastic foundation. the simplified continuum approach," *Buletinul Institutului Politehnic din Iasi*, vol. LV (LIX), no. 4, pp. 37–46, 2009.

[15] W. Shen and C. Teh, "Analysis of laterally loaded pile groups using a variational approach," *Geotechnique*, vol. 52, no. 3, pp. 201–208, 2002.

[16] A. P. Selvadurai, *Elastic analysis of soil-foundation interaction*. Elsevier, 2013.

[17] K. Terzaghi, "Evaluation of coefficients of subgrade reaction: Geotechnique," 1955.

[18] P. W. Rowe, "A theoretical and experimental analysis of sheet-pile walls," *Proceedings of the Institution of Civil Engineers*, vol. 4, no. 1, pp. 32–69, 1955.

[19] X. Karatzia and G. Mylonakis, "Horizontal stiffness and damping of piles in inhomogeneous soil," *Journal of Geotechnical and Geoenvironmental Engineering*, vol. 143, no. 4, p. 04016113, 2017.

[20] X. Karatzia and G. Mylonakis, "Horizontal response of piles in inhomogeneous soil: Simple analysis," in *Proceedings of the Second International Conference on Performance-Based Design in Earthquake Geotechnical Engineering, Taormina, Italy. Paper*, no. 1117, 2012.

[21] G. Mylonakis, *Contributions to static and seismic analysis of piles and pile-supported bridge piers*. State University of New York at Buffalo, 1995.

[22] M. Shadlou and S. Bhattacharya, "Dynamic stiffness of monopiles supporting offshore wind turbine generators," *Soil Dynamics and Earthquake Engineering*, vol. 88, pp. 15–32, 2016.

[23] B. Chen, X. Lu, P. Li, and Y. Chen, "Modeling of dynamic soil-structure interaction by ansys program," *Earthquake engineering and engineering vibration*, vol. 22, no. 1, pp. 126–131, 2002.

[24] L. Gao and S. Ye, "Numerical simulation of single pile static load test based on abaqus software," *Journal of Hebei University of Engineering (NATURAL SCIENCE EDITION)*, vol. 32, no. 03, pp. 51–54, 2015.

[25] M. Nikodỳm and K. Frydrỳšek, "Finite difference method used for the beams on elastic foundation-part 2 (applications)," 2012.

[26] L. C. Reese and W. F. Van Impe, *Single piles and pile groups under lateral loading*. CRC press, 2000.

[27] L. Auersch, "Compliance and damping of piles for wind tower foundation in non-homogeneous soils by the finite-element boundary-element method," *Soil Dynamics and Earthquake Engineering*, vol. 120, pp. 228–244, 2019.

[28] R. T. Corrêa, A. P. da Costa, and F. Simões, "Finite element modeling of a rail resting on a winkler-coulomb foundation and subjected to a moving concentrated load," *International Journal of Mechanical Sciences*, vol. 140, pp. 432–445, 2018.

[29] G. Tsiatas, "Nonlinear analysis of non-uniform beams on nonlinear elastic foundation," *Acta Mechanica*, vol. 209, pp. 141–152, 01 2010.

[30] S.-M. Kim, "Vibration and stability of axial loaded beams on elastic foundation under moving harmonic loads," *Engineering Structures*, vol. 26, no. 1, pp. 95–105, 2004.

[31] D. Basu, R. Salgado, and M. Prezzi, "A continuum-based model for analysis of laterally loaded piles in layered soils," *Geotechnique*, vol. 59, no. 2, pp. 127–140, 2009.

[32] M. Budhu and T. G. Davies, "Analysis of laterally loaded piles in soft clays," *Journal of Geotechnical Engineering*, vol. 114, no. 1, pp. 21–39, 1988.

[33] M. Hetényi and M. I. Hetbenyi, *Beams on elastic foundation: theory with applications in the fields of civil and mechanical engineering*, vol. 16. University of Michigan press Ann Arbor, MI, 1946.

[34] A. D. Kerr, "Elastic and viscoelastic foundation models," *Journal of Applied Mechanics, Transactions ASME*, vol. 31, no. 3, pp. 491–498, 1964.

[35] B. P. Rocha, R. A. Rodrigues, and H. L. Giacheti, "The flat dilatometer test in an unsaturated tropical soil site," *Geotechnical and Geological Engineering*, vol. 39, no. 8, pp. 5957–5969, 2021.

[36] H. Choo, W. Lee, S.-J. Hong, and C. Lee, "Application of the dilatometer test for estimating undrained shear strength of busan new port clay," *Ocean Engineering*, vol. 115, pp. 39–47, 2016.

[37] L. Cao, M.-F. Chang, and C. I. Teh, "Analysis of dilatometer test in clay," in *Proceedings of the 3rd International Conference on the Flat Dilatometer (DMT'15), Roma, Italy*, pp. 14–16, 2015.

[38] F. Schnaid, E. Odebrecht, J. Sosnoski, and P. Robertson, "Effects of test procedure on flat dilatometer test (dmt) results in intermediate soils," *Canadian Geotechnical Journal*, vol. 53, no. 8, pp. 1270–1280, 2016.

[39] S. Rabarijoely, "Dilatometer test calibrations for evaluating soil parameters," *Acta Scientiarum Polonorum. Architectura*, vol. 20, no. 3, 2021.

[40] G. Zhang, C. Li, S. Xiao, Y. Guo, Z. Cao, and Y. Liu, "Investigation of in situ thermomechanical behaviors of soil around an energy pile with flat dilatometer tests," *Acta Geotechnica*, pp. 1–15, 2021.

[41] G. K. Martin and P. W. Mayne, "Seismic flat dilatometer tests in connecticut valley varved clay," *Geotechnical Testing Journal*, vol. 20, pp. 357–361, 1997.

[42] S. M. Ahmed, "Assessment of clay stiffness and strength parameters using index properties," *Journal of Rock Mechanics and Geotechnical Engineering*, vol. 10, no. 3, pp. 579–593, 2018.

[43] S. M. Ahmed and S. S. Agaiby, "Strength and stiffness characterization of clays using atterberg limits," *Transportation Geotechnics*, vol. 25, p. 100420, 2020.

[44] A. Aloisio, F. Totani, and G. Totani, "Experimental dispersion curves of non-penetrable soils from direct dynamic measurements using the seismic dilatometer (sdmt)," *Soil Dynamics and Earthquake Engineering*, vol. 143, p. 106616, 2021.

[45] R. Lancellotta, *Geotechnical engineering*. CRC Press, 2008.

[46] S. M. Toolbox *et al.*, "Matlab," *Mathworks Inc*, 1993.

[47] W. R. Inc., "Mathematica." Champaign, IL, 2021.

[48] D. Froio and E. Rizzi, "Analytical solution for the elastic bending of beams lying on a linearly variable winkler support," *International Journal of Mechanical Sciences*, vol. 128, pp. 680–694, 2017.

[49] K. Terzaghi, "Evalution of conefficients of subgrade reaction," *Geotechnique*, vol. 5, no. 4, pp. 297–326, 1955.

[50] G. Anoyatis and A. Lemnitzer, "Dynamic pile impedances for laterally–loaded piles using improved tajimi and winkler formulations," *Soil Dynamics and Earthquake Engineering*, vol. 92, pp. 279–297, 2017.

[51] L. J. Prendergast and K. Gavin, "A comparison of initial stiffness formulations for small-strain soil–pile dynamic winkler modelling," *Soil Dynamics and Earthquake Engineering*, vol. 81, pp. 27–41, 2016.

[52] H. Hirai, "Analysis of piled raft with nodular pile subjected to vertical load using a winkler model approach," *International Journal for Numerical and Analytical Methods in Geomechanics*, vol. 40, no. 13, pp. 1863–1889, 2016.

[53] S. Timoshenko, "Method of analysis of statical and dynamical stresses in rail," *Proceedings of the 2nd International Congress for Applied Mechanics, vol. 54, pp. 1–12. Zurich, Switzerland*, 1927.

[54] M. Biot, "Bending of an infinite beam on an elastic foundation," *J. Appl. Mech. Trans. ASME 59(203), 1–7*, 1937.

[55] M. Shadlou and S. Bhattacharya, "Dynamic stiffness of pile in a layered elastic continuum," *Geotechnique*, vol. 64, no. 4, pp. 303–319, 2014.

[56] M. Filonenko-Borodich, "Some approximate theories of elastic foundation," *Uchenyie Zapiski Moskovkogo Gosudarstuennogo Universiteta Mekhanika, Moscow*, vol. 46, pp. 3–18, 1940.

[57] M. Hetenyi, "Beams and plates on elastic foundations and related problems," *Applied Mechanics Reviews*, vol. 19, no. 2, pp. 95–102, 1966.

[58] C. P. Filipich and M. B. Rosales, "A further study about the behaviour of foundation piles and beams in a winkler-pasternak soil," *International Journal of Mechanical Sciences*, vol. 44, no. 1, pp. 21–36, 2002.

[59] V. Vlasov and U. Leontiev, "Beams plates and shells on elastic foundations israel programme for scientific translations," *Jerusalem: Israel Program for Scientific Translations*, 1966.

[60] K. Hayashi *Theorie des Tragers Auf Elastischer Unterlage und Ihre Anwendung Auf den Tiefbau*, 1921.

[61] A. Hendry, "New method for the analysis of beams on elastic foundations," *Civ. Eng. Public Works Rev. 53(621), 297– 299*, 1958.

[62] K. Iyengar and S. Anantharamu, "Finite beam-columns on elastic foundations," *J. Eng. Mech. Div. Proc. ASCE 89(EM6), 139–160*, 1963.

[63] K. Iyengar and S. Anantharamu, "Influence lines for beams on elastic foundations," *J.*

Struct.Div. Proc.ASCE91(ST3), 45–56, 1965.

[64] J. N. Franklin and R. F. Scott, "Beam equation with variable foundation coefficient," *ASCE J Eng Mech Div*, vol. 105, no. 5, pp. 811–827, 1979.

[65] M. Lentini, "Numerical solution of the beam equation with nonuniform foundation coefficient.," *Journal of Applied Mechanics, Transactions ASME*, vol. 46, no. 4, pp. 750–756, 1979.

[66] J. Clastornik, M. Eisenberger, D. Z. Yankelevsky, and M. A. Adin, "Beams on variable winkler elastic foundation," *Journal of Applied Mechanics, Transactions ASME*, vol. 53, no. 4, pp. 925–928, 1986.

[67] D. Froio, R. G. Moioli, and E. Rizzi, "Numerical dynamic analysis of beams on nonlinear elastic foundations under harmonic moving load," in *ECCOMAS 2016: 7th European Congress on Computational Methods in Applied Sciences and Engineering, Crete Island, Greece, 5-10 June 2016*, pp. 4784–4809, NTUA (National Technical University of Athens), 2016.

[68] M. B. Darendeli, *Development of a new family of normalized modulus reduction and material damping curves*. The university of Texas at Austin, 2001.

[69] D. Froio and E. Rizzi, "Analytical solution for the elastic bending of beams lying on a variable winkler support," *Acta Mechanica*, vol. 227, no. 4, pp. 1157–1179, 2016.

[70] J. Fradelos, "Pail stiffness matrix in homogeneous and inhomogeneous soil under transverse loading," *PhD. Thesis*, no. University of Patras, 2016.

[71] J.J.Crispin, "Flexural elastic response of single piles in inhomogeneous soil," *Research report No. 1617RP005M*, vol. Department of Civil Engineering, no. University of Bristol, p. UK, 2017.

[72] H. Parashakis, *Stress Wave Propagation in Inhomogeneous Soil Media*. University of Patras, Greece, 2020.

[73] D. C. Rosendo and P. J. Albuquerque, "General analytical solution for laterally-loaded pile-based miche model," *Geotechnical and Geological Engineering*, vol. 39, no. 2, pp. 765–782, 2021.

[74] M. R. Madhav, N. S. V. K. Rao, and K. Madhavan, "Laterally loaded pile in elasto-plastic soil," *SOILS AND FOUNDATIONS*, vol. 11, no. 2, pp. 1–15, 1971.

[75] M. F. Randolph, "The response of flexible piles to lateral loading," *Geotechnique*, vol. 31, no. 2, pp. 247–259, 1981.

[76] F. W. Olver, D. W. Lozier, R. F. Boisvert, and C. W. Clark, *NIST handbook of mathematical functions hardback and CD-ROM*. Cambridge university press, 2010.

[77] R. Di Laora, A. Mandolini, and G. Mylonakis, "Insight on kinematic bending of flexible piles in layered soil," *Soil Dynamics and Earthquake Engineering*, vol. 43, pp. 309–322, 2012.

[78] G. P. Cavinato, C. Carusi, M. Dall'Asta, E. Miccadei, and T. Piacentini, "Sedimentary and tectonic evolution of plio–pleistocene alluvial and lacustrine deposits of fucino basin (central italy)," *Sedimentary Geology*, vol. 148, no. 1-2, pp. 29–59, 2002.

[79] S. Marchetti, "In situ tests by flat dilatometer," *Journal of the geotechnical engineering division*, vol. 106, no. 3, pp. 299–321, 1980.

[80] Z. Lechowicz, M. Fukue, S. Rabarijoely, and M. J. Sulewska, "Evaluation of the undrained shear strength of organic soils from a dilatometer test using artificial neural networks," *Applied Sciences*, vol. 8, no. 8, p. 1395, 2018.

[81] C. Ferreira, A. Viana da Fonseca, C. Ramos, A. S. Saldanha, S. Amoroso, and C. Rodrigues, "Comparative analysis of liquefaction susceptibility assessment methods based on the investigation on a pilot site in the greater lisbon area," *Bulletin of Earthquake Engineering*, vol. 18, no. 1, pp. 109–138, 2020.

[82] E. Pavithra, "Dilatometric methods: Insights of other researchers," in *IOP Conference Series: Materials Science and Engineering*, vol. 923, p. 012041, IOP Publishing, 2020.

[83] A. Erdélyi *Higher Transcendental Functions*, 1953.

[84] W. F. Trench, "Elementary differential equations with boundary value problems," 2013.

Appendix A.

This section is devoted to the determination of the unique solution of the BVP given by Eq.(3) and Eq.(9). The whole mathematical formulation has been described herein for completeness purposes.

Appendix A.1. The general integral of Eq.(3)

In order to provide a general solution for Eq.(3), a suitable change of variable $s = s(x)$ is adopted which allows, as shown in the following paragraphs, to write Eq.(3) in the following form:

$$\sum_{k=1}^{4} s^k \tilde{v}^{(k)}(s) = s\tilde{v}(s), \tag{A.1}$$

or, in a more generic form, as

$$s^{q+1}\tilde{v}^{(q+1)}(s) + \sum_{k=1}^{q} s^{k-1}(\alpha_k s + \beta_k)\tilde{v}^{(k)}(s) + \alpha_0 \tilde{v}(s) = 0, \tag{A.2}$$

where each derivative is compensated by the corresponding power of the variable. Finally, by applying an additional change of variable $t = t(s)$, Eq.(A.2) can be

written as a generalized hypergeometric equation

$$\left[\frac{d}{dt}\left(t\frac{d}{dt}+b_1-1\right)\left(t\frac{d}{dt}+b_2-1\right)...\left(t\frac{d}{dt}+b_q-1\right)+\right.$$
$$\left.-\left(t\frac{d}{dt}+a_1\right)\left(t\frac{d}{dt}+a_2\right)...\left(t\frac{d}{dt}+a_p\right)\right]w(t)=0, \tag{A.3}$$

with $p,q\in\mathbb{N}$ and $a_1,\ldots,a_p,b_1,\ldots,b_q\in\mathbb{R}$. In the case of null index $p=0$, i.e. when the set of factors $t\frac{d}{dt}+a_i$ is empty, we shall replace such empty product by the identity operator 1, so that the expression in Eq.(A.3) can be written as

$$\left[\frac{d}{dt}\left(t\frac{d}{dt}+b_1-1\right)\left(t\frac{d}{dt}+b_2-1\right)...\left(t\frac{d}{dt}+b_q-1\right)-1\right]w(t)=0. \tag{A.4}$$

Eq.(A.4) is a generalized hypergeometric differential equation whose general integral can be expressed by a linear combination of linearly independent *generalized hypergeometric functions* depending on the parameters b_j, $1\leq j\leq q$, see [83]. For the forthcoming analytical developments, it is worthwhile to introduce at this stage the generalized hypergeometric function ${}_pF_q(\bar{a};\bar{b};\cdot)$ depending on the parameters $\bar{a}:=(a_1,...,a_p)\in\mathbb{R}^p$ and $\bar{b}:=(b_1,...,b_q)\in\mathbb{R}^q$, appearing in Eq.(A.3) and respectively called numerator and denominator parameters, defined by setting

$${}_pF_q(\bar{a};\bar{b};t)={}_pF_q(a_1,...,a_p;b_1,...,b_q;t)=1+\sum_{h=1}^{\infty}\frac{\prod_{i=1}^{p}(a_i)_h t^h}{\prod_{j=1}^{q}(b_j)_h h!}, \tag{A.5}$$

where, to denote the increasing factorial to h factors of a real number c, the Pochhammer symbol has been used, i.e.

$$(c)_h=c(c+1)\cdots(c+h-1)=\frac{\Gamma(c+h)}{\Gamma(c)} \tag{A.6}$$

where $\Gamma(\cdot)$ is Euler's Gamma function which generalizes the factorial to $\mathbb{R}$. By explicitly writing the product in Eq.(A.5) we get

$${}_pF_q(\bar{a};\bar{b};t)=\sum_{h=0}^{\infty}\frac{(a_1)_h(a_2)_h\cdots(a_p)_h}{(b_1)_h(b_2)_h\cdots(b_q)_h}\frac{t^h}{h!}. \tag{A.7}$$

It might be worth to remark that the function ${}_pF_q$ does not depend on the order into which the components of the vectors $\bar{a} \in \mathbb{R}^p$ and $\bar{b} \in \mathbb{R}^q$ appear. The series in Eq.(A.7) is characterized by the following properties:

i) is convergent $\forall t$ if $p \leq q$;

ii) is convergent $\forall t \in \mathbb{R}, |t| \leq 1$ if $p = q + 1$;

iii) is divergent if $p > q + 1$.

The function ${}_pF_q(\bar{a}; \bar{b}; \cdot)$ is, unless special cases in the choice of numerator and denominator parameters, the unique solution of Eq.(A.3) which is bounded in a neighbourhood of $t = 0$. When none of the values b_j is a positive integer and none of the differences $b_j - b_i$ is an integer number, the functions w_k defined by setting

$$w_k(t) := \begin{cases} {}_pF_q(\bar{a}; \bar{b}; t) = {}_pF_q(a_1, ..., a_p; b_1, ..., b_q; t) \\ \qquad\qquad \text{if } k = 0, \\ |t|^{1-b_k} {}_pF_q(1 + a_1 - b_k, ..., 1 + a_p - b_k; 2 - b_k, 1 + b_1 - b_k, ..., 1 + b_q - b_k; t) \\ \qquad\qquad \text{if } 1 \leq k \leq q, \end{cases} \tag{A.8}$$

provide a system, $(w_k)_{0 \leq k \leq q}$, of $q + 1$ independent solutions to Eq.(A.3). To this regard we warn the reader that the habit, present in the literature, to solve Eq.(A.3) in $\mathbb{R}_+$ has lost the information related to the presence of the absolute value on the variable t in the definition of the solutions w_k, see [84]. It might also be worth to remark that the parameters a_i and b_j which are present in the expression which defines w_0 are replaced by $1 + a_i - b_k$ and, respectively, by $1 + b_j - b_k$ when $j \neq k$ and by $2 - b_k$ if $j = k$. Complying with our case study, where $p = 0$ and $q = 3$, Eq.(A.4), which can be written in a compact form by introducing the differential operator $\delta = t\frac{d}{dt}$ as

$$[\delta(\delta + b_1 - 1) \cdot (\delta + b_2 - 1)(\delta + b_3 - 1) - t]w(t) = 0, \tag{A.9}$$

admits as fundamental system of solutions the functions w_k, $k \in \{0, 1, 2, 3\}$, defined by Eq.(8). Therefore, the general integral of Eq.(A.9), also called complementary

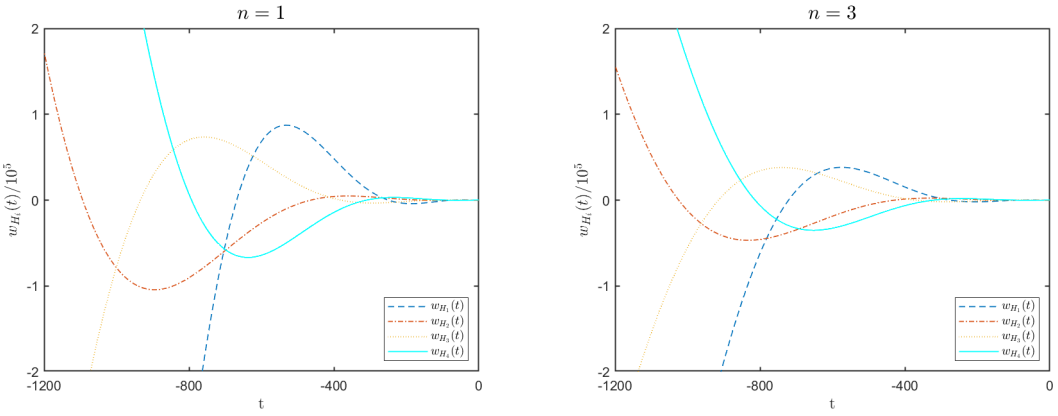

Figure A.7: Fundamental set of solutions of Eq. (A.9) for $n = 1$ and $n = 3$.

function, if it exists, is given by the linear combination

$$w(t) = \sum_{k=0}^{3} c_k w_k(t) \tag{A.10}$$

of the four linearly independent functions $w_k(t)$, given by Eq.(8), with coefficients c_0, c_1, c_2, c_3, which will be determined by imposing the boundary conditions prescribed at the top and the bottom of the beam.

In order to determine the values of the denominator parameters $(b_j)_{1\leq j\leq 3}$ which affect the general integral Eq.(A.10) we give here the details of suitable changes of variable which allow to transform Eq.(2) into Eq.(A.4). Set

$$\gamma := (EJk_1^4)^{\frac{1}{n+4}}, \tag{A.11}$$

since $k_1 \neq 0$ (see Eq.(6)), the following variable transformation is invertible

$$s = s(x) = \frac{k_0 + k_1 x}{\gamma} \iff x = x(s) = \frac{\gamma s - k_0}{k_1} \tag{A.12}$$

and maps the interval $[0, L]$ into the interval with extremes $\frac{k_0}{\gamma}$ and $\frac{k_0+k_1 L}{\gamma}$. Then, the substrate stiffness takes the following expression

$$K(x) = (k_0 + k_1 x)^n = s^n \gamma^n. \tag{A.13}$$

Setting

$$\tilde{v}(s) = v(x(s)) = v\left(\frac{\gamma s - k_0}{k_1}\right) \tag{A.14}$$

we get that

$$v^{(4)}(x) = \tilde{v}^{(4)}(s(x))\left(\frac{ds(x)}{dx}\right)^4 = \left(\frac{k_1}{\gamma}\right)^4 v^{(4)}(s). \tag{A.15}$$

Then, by replacing Eqs.(A.15) and (A.13) in Eq.(3) one gets

$$EJ\left(\frac{k_1}{\gamma}\right)^4 \tilde{v}^{(4)}(s) + \gamma^n s^n \tilde{v}(s) = 0, \tag{A.16}$$

hence, by dividing for γ^n, the following holds:

$$\left(\frac{EJk_1^4}{\gamma^{n+4}}\right)^4 \tilde{v}^{(4)}(s) + s^n \tilde{v}(s) = 0. \tag{A.17}$$

So, by using Eq.(A.11), the differential equation (A.17) can be written as

$$s^4 \tilde{v}^{(4)}(s) + s^{n+4}\tilde{v}(s) = 0. \tag{A.18}$$

At this stage, by introducing the negative parameter $t(s)$,

$$t = t(s) = -\frac{s^{n+4}}{(n+4)^4} \iff s = s(t) = (-(n+4)^4 t)^{\frac{1}{n+4}}, \tag{A.19}$$

fully-defined in the intervals with extremes $-\frac{1}{(n+4)^4}\left(\frac{k_0}{\gamma}\right)^{n+4}$ and $-\frac{1}{(n+4)^4}\left(\frac{k_0+k_1 L}{\gamma}\right)^{n+4}$,
and by setting

$$w(t) = \tilde{v}(s(t)) = \tilde{v}((-(n+4)^4 t)^{\frac{1}{n+4}}), \tag{A.20}$$

since

$$\frac{ds(t)}{dt} = \frac{d}{dt}\left(-(n+4)^4 t\right)^{\frac{1}{n+4}} = -(n+4)^{-\frac{n}{n+4}}(-t)^{-\frac{n+3}{n+4}},$$

one gets that

$$
\begin{aligned}
\tilde{v}^{(1)}(s) &= -(n+4)^{\frac{n}{n+4}}(-t)^{\frac{n+3}{n+4}}w^{(1)}(t),\\
\tilde{v}^{(2)}(s) &= (n+4)^{\frac{2n}{n+4}}(-t)^{2\frac{n+3}{n+4}}w^{(2)}(t)+\\
&\quad -(n+3)(n+4)^{\frac{n-4}{n+4}}(-t)^{\frac{n+2}{n+4}}w^{(1)}(t),\\
\tilde{v}^{(3)}(s) &= -(n+4)^{\frac{3n}{n+4}}(-t)^{3\frac{n+3}{n+4}}w^{(3)}(t)+\\
&\quad +3(n+3)(n+4)^{2\frac{n-2}{n+4}}(-t)^{\frac{2n+5}{n+4}}w^{(2)}(t)+\\
&\quad -(n+2)(n+3)(n+4)^{\frac{n-8}{n+4}}(-t)^{\frac{n+1}{n+4}}w^{(1)}(t),\\
\tilde{v}^{(4)}(s) &= (n+4)^{\frac{4n}{n+4}}(-t)^{\frac{4n+12}{n+4}}w^{(4)}(t)+\\
&\quad -6(n+3)(n+4)^{\frac{3n-4}{n+4}}(-t)^{\frac{3n+8}{n+4}}w^{(3)}(t)+\\
&\quad +(7n+17)(n+3)(n+4)^{\frac{2n-8}{n+4}}(-t)^{\frac{2n+4}{n+4}}w^{(2)}(t)+\\
&\quad (n+1)(n+2)(n+3)(n+4)^{\frac{n-12}{n+4}}(-t)^{\frac{n}{n+4}}w^{(1)}(t).
\end{aligned}
$$

873 Then, by replacing the above relation in Eq.(A.18), after proper manipulations, one
874 gets the following expression

$$
\begin{aligned}
t^4w^{(4)}(t) + 6\frac{n+3}{n+4}t^3w^{(3)}(t) + \frac{(n+3)(7n+17)}{(n+4)^2}t^2w^{(2)}(t)+\\
+\frac{(n+1)(n+2)(n+3)}{(n+4)^3}tw^{(1)}(t) - tw(t) = 0.
\end{aligned}
\tag{A.21}
$$

875 Then, one gets that Eq.(A.21) can be expressed by Eq.(A.9), if and only if (b_1, b_2, b_3)
876 is a solution of the following system:

$$
\begin{cases}
b_1 + b_2 + b_3 + 3 = 6\frac{n+3}{n+4}\\
1 + b_1b_3 + b_2 + b_1b_2 + b_1b_3 + b_2b_3 = \frac{(n+3)(7n+17n)}{(n+4)^2}\\
b_1b_2b_3 = \frac{(n+1)(n+2)(n+3)}{(n+4)^3}.
\end{cases}
\tag{A.22}
$$

877 The system in Eq.(A.22) admits 3! solutions which are the 3! permutations of the
878 components

$$
b_j = \frac{n+j}{n+4}, \qquad 1 \le j \le 3, \tag{A.23}
$$

of the vector $\bar{b} = (b_1, b_2, b_3)$ which, as already remarked, do not affect the value of the functions ${}_0F_3(-;\bar{b};\cdot)$. Therefore, from now on we shall assume that the denominator parameters b_j, $1 \leq j \leq 3$ are determined using the formula in Eq.(A.23). Then, since $n \in \mathbb{N} \setminus \{0\}$, none of the parameters b_j is a positive integer and none of the differences $b_j - b_i = \frac{j-i}{n+4}$ is an integer number, so the functions w_k, defined by Eq.(8), determine a fundamental system of solution of Eq.(A.9). By including the two invertible changes of variable produced by Eq.(A.12) and Eq.(A.19), one gets, by using also Eq.(A.11), that

$$x = x(t) = \frac{[EJk_1^4(n+4)]^{\frac{1}{n+4}}\,(-t)^{\frac{1}{n+4}} - k_0}{k_1} \quad \Leftrightarrow \quad t = t(x) = -\frac{1}{(n+4)^4}\left(\frac{k_0 + k_1 x}{EJk_1^4}\right)^{n+4}.$$

Therefore, by using Eq.(A.10), the general integral of Eq.(3) is obtained as the following linear combination of independent functions in the variable x:

$$\begin{aligned} v(x) = \tilde{v}(s) &= w\left(-\frac{s^{n+4}}{(n+4)^4}\right) = w\left(-\frac{(k_0+k_1x)^{n+4}}{\gamma^{n+4}(n+4)^4}\right) \\ &= \sum_{k=0}^{3} c_k w_k\left(-\frac{1}{(n+4)^4}\frac{(k_0+k_1x)^{n+4}}{EJk_1^4}\right). \end{aligned} \tag{A.24}$$

Appendix A.2. The solution of the BVP Eq.s (3)-(9)

Now we show how to determine the constants c_0, c_1, c_2, c_3 in Eq.(7) once the boundary conditions Eq.(3.1.2) are prescribed. Such conditions, expressed in terms of the variable $s = s(x)$ defined by Eq.(A.12), become

$$\begin{cases} \tilde{v}^{(2)}(\frac{k_0}{\gamma})(\frac{k_1}{\gamma})^2 = -\frac{W}{EJ} \\ \tilde{v}^{(3)}(\frac{k_0}{\gamma})(\frac{k_1}{\gamma})^3 = -\frac{F}{EJ} \\ \tilde{v}^{(2)}(\frac{k_0+k_1L}{\gamma})(\frac{k_1}{\gamma})^2 = 0 \\ \tilde{v}^{(3)}(\frac{k_0+k_1L}{\gamma})(\frac{k_1}{\gamma})^3 = 0. \end{cases} \tag{A.25}$$

By substituting Eq.(11) in Eq.(A.11) one gets

$$\gamma := \left[\frac{EJ}{L^4}\,(\alpha\beta^n)^{\frac{4}{n+4}}\right]^{\frac{1}{n}}. \tag{A.26}$$

It is worth to remark that the oddness assumption of n is introduced just to investigate also the case $\beta < 0$. Then, by easy manipulations, we get that k_0 and k_1 can be expressed in terms of α and β so that:

$$k_0 = \alpha^{\frac{1}{n+4}} \beta^{\frac{-4}{n+4}} \gamma \quad \Rightarrow \quad \frac{k_0}{\gamma} = \left(\frac{\alpha}{\beta^4}\right)^{\frac{1}{n+4}}, \tag{A.27}$$

$$k_1 = \frac{1}{L} \alpha^{\frac{1}{n+4}} \beta^{\frac{n}{n+4}} \gamma \quad \Rightarrow \quad \frac{k_1 L}{\gamma} = (\alpha \beta^n)^{\frac{1}{n+4}}. \tag{A.28}$$

In particular, the following equality holds

$$\frac{k_0 + k_1 L}{\gamma} = \left(\frac{\alpha}{\beta^4}\right)^{\frac{1}{n+4}} (1+\beta). \tag{A.29}$$

In this way, by replacing (A.27) and (A.29) into the set of boundary conditions (A.25) one gets

$$\begin{cases} \tilde{v}^{(2)}\left(\left(\frac{\alpha}{\beta^4}\right)^{\frac{1}{n+4}}\right) = -\frac{W}{EJ}\left(\frac{L}{(\alpha\beta^n)^{\frac{1}{n+4}}}\right)^2 \\ \tilde{v}^{(3)}\left(\left(\frac{\alpha}{\beta^4}\right)^{\frac{1}{n+4}}\right) = -\frac{F}{EJ}\left(\frac{L}{(\alpha\beta^n)^{\frac{1}{n+4}}}\right)^3 \\ \tilde{v}^{(2)}\left(\left(\frac{\alpha}{\beta^4}\right)^{\frac{1}{n+4}}(1+\beta)\right) = 0 \\ \tilde{v}^{(3)}\left(\left(\frac{\alpha}{\beta^4}\right)^{\frac{1}{n+4}}(1+\beta)\right) = 0, \end{cases} \tag{A.30}$$

where $\tilde{v}(s) = w\left(-\frac{s^{n+4}}{(n+4)^4}\right)$ is obtained as linear combination, with coefficients c_0, c_1, c_2, c_3, of the independent integrals $\tilde{v}_k(s) = w_k\left(-\frac{s^{n+4}}{(n+4)^4}\right)$ with $0 \le k \le 3$ given by Eq.(A.9). Due to the linearity of the derivative operator, the BC in Eq.(A.30) can be expressed in vector form as:

$$[B] \cdot \bar{c} = \bar{f}_F + \bar{f}_W \tag{A.31}$$

where, taking into account the identities in Eq.(A.28) and Eq.(A.29),

$$[B] = \begin{pmatrix} \tilde{v}_0^{(2)}(\frac{k_0}{\gamma}) & \tilde{v}_1^{(2)}(\frac{k_0}{\gamma}) & \tilde{v}_2^{(2)}(\frac{k_0}{\gamma}) & \tilde{v}_3^{(2)}(\frac{k_0}{\gamma}) \\ \tilde{v}_0^{(3)}(\frac{k_0}{\gamma}) & \tilde{v}_1^{(3)}(\frac{k_0}{\gamma}) & \tilde{v}_2^{(3)}(\frac{k_0}{\gamma}) & \tilde{v}_3^{(3)}(\frac{k_0}{\gamma}) \\ \tilde{v}_0^{(2)}(\frac{k_0+k_1L}{\gamma}) & \tilde{v}_1^{(2)}(\frac{k_0+k_1L}{\gamma}) & \tilde{v}_2^{(2)}(\frac{k_0+k_1L}{\gamma}) & \tilde{v}_3^{(2)}(\frac{k_0+k_1L}{\gamma}) \\ \tilde{v}_0^{(3)}(\frac{k_0+k_1L}{\gamma}) & \tilde{v}_1^{(3)}(\frac{k_0+k_1L}{\gamma}) & \tilde{v}_2^{(3)}(\frac{k_0+k_1L}{\gamma}) & \tilde{v}_3^{(3)}(\frac{k_0+k_1L}{\gamma}) \end{pmatrix} \tag{A.32}$$

and

$$\bar{c} = \begin{pmatrix} c_0 \\ c_1 \\ c_2 \\ c_3 \end{pmatrix} \in \mathbb{R}^4$$

is the vector of the unknown coefficients c_k, $0 \leq k \leq 3$, on which the general integral (A.24) of Eq.(3) rely. Finally, the vector $\bar{f}$ describing the constant terms is given by the sum $\bar{f} = \bar{f}_F + \bar{f}_W$ where

$$\bar{f}_F = \frac{FL^3}{(\alpha\beta^n)^{\frac{3}{n+4}}EJ} \begin{pmatrix} 0 \\ -1 \\ 0 \\ 0 \end{pmatrix} \in \mathbb{R}^4, \qquad \bar{f}_W = \frac{WL^2}{(\alpha\beta^n)^{\frac{2}{n+4}}EJ} \begin{pmatrix} -1 \\ 0 \\ 0 \\ 0 \end{pmatrix} \in \mathbb{R}^4. \tag{A.33}$$

Then, under the no-singularity condition of $[B]$, equation (A.31) admits a unique solution $\bar{c}$ which determines the unique solution of the Boundary Value Problem (BVP) given by the differential equation (3) and the boundary conditions Eq.(9) (or, equivalently, Eq.(A.30)).

To provide a complete understanding of the behaviour of the beam-foundation system, by taking advantage of the linearity of Eq.(A.31), the superposition principle may be applied to decompose the response into two contributions. Each contribution refers to the independent action of the force F or of the moment W, respectively. Therefore, it is possible to split the linear system (A.31) into two subsystems, the first with $F \neq 0$ and $W = 0$, and the second with $F = 0$ and $W \neq 0$. Then, set

$$\bar{c}_F = [B]^{-1} \cdot \bar{f}_F \quad \text{and} \quad \bar{c}_W = [B]^{-1} \cdot \bar{f}_W, \tag{A.34}$$

when both F and W are nontrivial, the vector $\bar{c} = \bar{c}_F + \bar{c}_W$ gives the unique solution of Eq.(A.31). Eventually, by replacing the components of the vector $\bar{c} = (c_0, c_1, c_2, c_3)$ in Eq.(A.24) one get the solution of BVP Eq.s(3) and (9).

Appendix B.

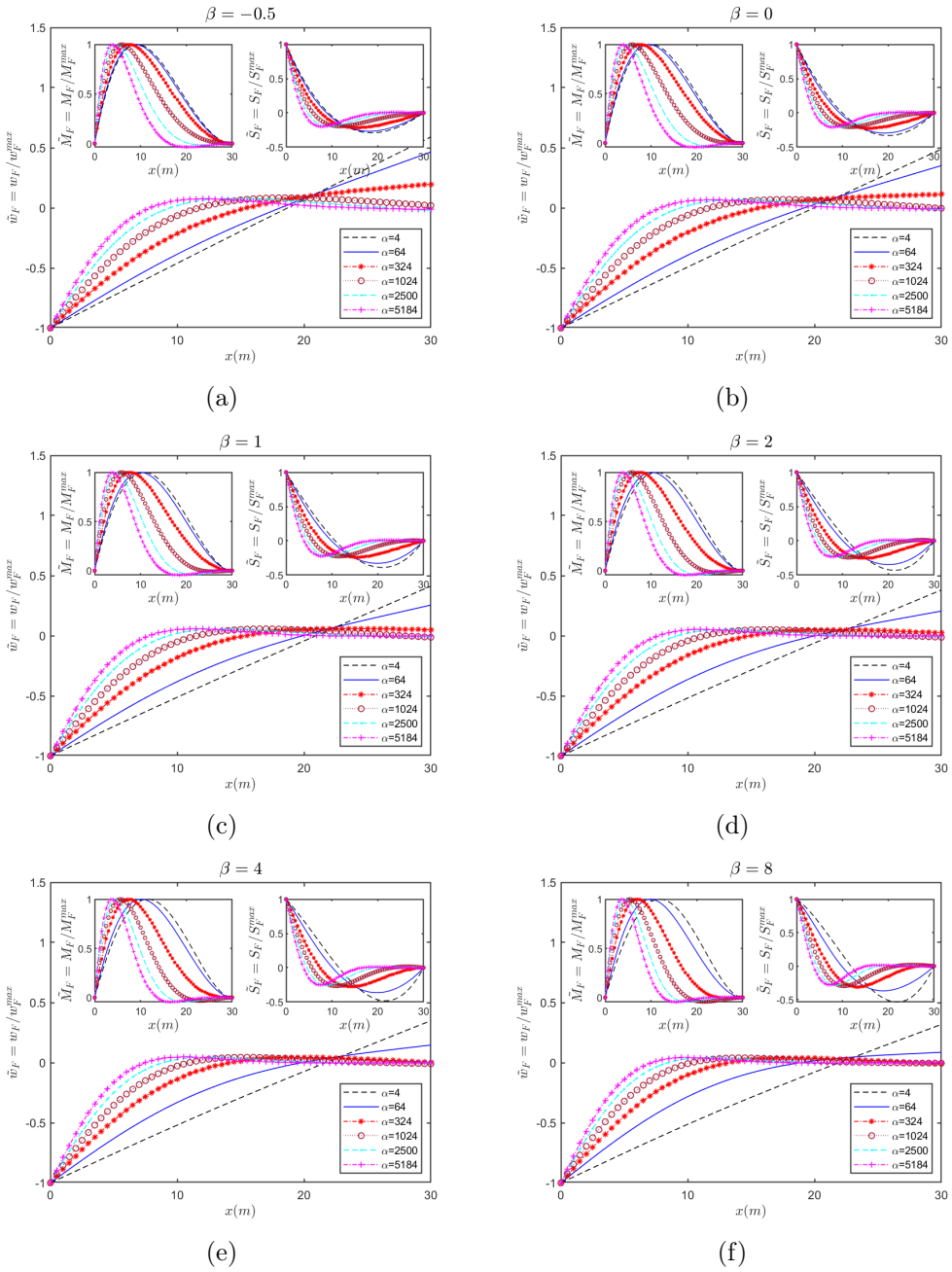

Figure B.8: Normalized shape of elastic deflection $\tilde{v}_F = v_F/v_F^{max}$, bending moment $\tilde{M}_F = M_F/M_F^{max}$ and shear $\tilde{S}_F = S_F/S_F^{max}$ for $n = 1$, under horizontal force F, for various values of α and β ($\beta = -0.5$ (a), $\beta \to 0$ (b), $\beta = 1$ (c), $\beta = 2$ (d), $\beta = 4$ (e), $\beta = 8$ (f)).α is representative of the ratio between the stiffness of the foundation, K_0, calculated at the top and of the beam, and the beam's bending stiffness E. As α approaches relatively high values, the beam longitudinal axis starts deforming more, conversely for low values of the same parameter stiff foundation is simulated.β is representative of the steepness of the elastic stiffness, k_1/k_0, coefficient variation along the beam axis. For positive higher value of β, stiff foundation property is achieved early with varying beam longitudinal axis. Negative value of this parameter simulates soft soil responses with decreasing stiffness of the elastic springs at increasing depth.

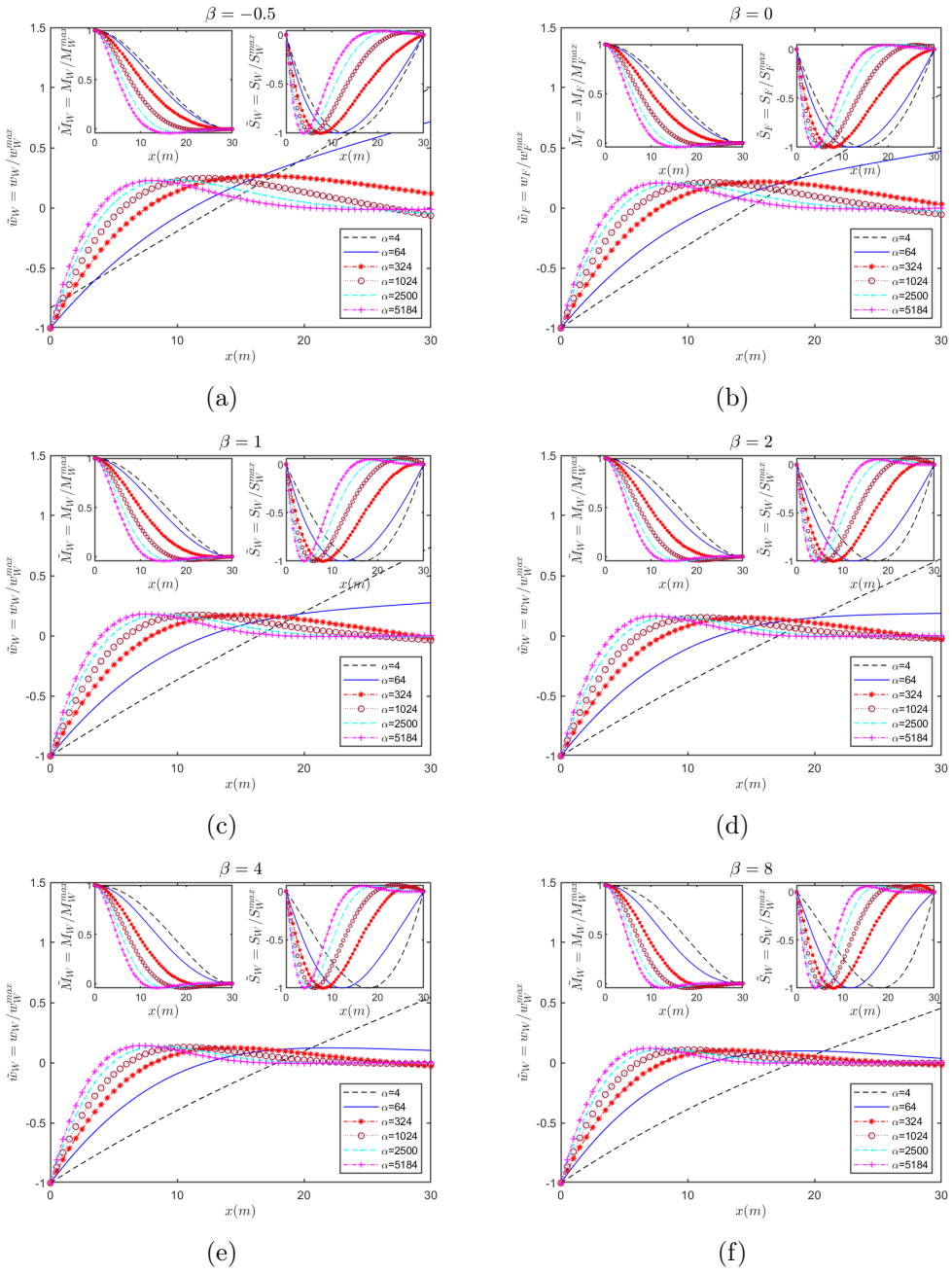

Figure B.9: Normalized shape of elastic deflection $\tilde{v}_W = v_W/v_W^{max}$, bending moment $\tilde{M}_W = M_W/M_W^{max}$ and shear $\tilde{S}_W = S_W/S_W^{max}$ for $n = 1$, under moment W, for various values of α and β ($\beta = -0.5$ (a), $\beta \to 0$ (b), $\beta = 1$ (c), $\beta = 2$ (d), $\beta = 4$ (e), $\beta = 8$ (f)).α is representative of the ratio between the stiffness of the foundation, K_0, calculated at the top and of the beam, and the beam's bending stiffness E. As α approaches relatively high values, the beam longitudinal axis starts deforming more, conversely for low values of the same parameter stiff foundation is simulated.β is representative of the steepness of the elastic stiffness, k_1/k_0, coefficient variation along the beam axis. For positive higher value of β, stiff foundation property is achieved early with varying beam longitudinal axis. Negative value of this parameter simulates soft soil responses with decreasing stiffness of the elastic springs at increasing depth.